







Fractional Einstein-Gauss-Bonnet scalar field cosmology

Bayron Micolta-Riascos ^{1,*} Alfredo D. Millano ^{2,†} Genly Leon ^{2,3,‡}
Byron Droguett ^{4,§} Esteban González ^{1,¶} and Juan Magaña ^{5,**}

¹*Departamento de Física, Universidad Católica del Norte,
Avenida Angamos 0610, Casilla 1280, Antofagasta, Chile*

²*Departamento de Matemáticas, Universidad Católica del Norte,
Avenida Angamos 0610, Casilla 1280 Antofagasta, Chile*

³*Institute of Systems Science, Durban University of Technology,
P.O. Box 1334, Durban 4000, Republic of South Africa*

⁴*Department of Physics, Universidad de Antofagasta, 1240000 Antofagasta, Chile*

⁵*Escuela de Ingeniería, Universidad Central de Chile,
Avenida Francisco de Aguirre 0405, 171-0164, La Serena Coquimbo, Chile*

(Dated: October 2, 2024)

Our paper introduces a new theory called Fractional Einstein-Gauss-Bonnet scalar field cosmology, which has significant implications for Cosmology. We derived a modified Friedmann equation and a modified Klein-Gordon equation using fractional calculus to modify the gravitational action integral. Our research reveals non-trivial solutions associated with exponential potential, exponential couplings to the Gauss-Bonnet term, and logarithmic scalar field, which are dependent on two cosmological parameters, m and $\alpha_0 = t_0 H_0$ and the fractional derivative order μ . By employing linear stability theory, we reveal the phase space structure and analyze the dynamic effects of the Gauss-Bonnet couplings. The scaling behavior at some equilibrium points reveals that the geometric corrections in the coupling to the Gauss-Bonnet scalar can mimic the behavior of the dark sector in modified gravity. Using data from cosmic chronometers, type Ia supernovae, supermassive black hole shadows, and strong gravitational lensing, we estimated the values of m and α_0 , indicating that the solution is consistent with an accelerated expansion at late times with the values $\alpha_0 = 1.38 \pm 0.05$, $m = 1.44 \pm 0.05$, and $\mu = 1.491$ (consistent with $\Omega_{m,0} = 0.311 \pm 0.016$ and $h = 0.712 \pm 0.007$), resulting in an age of the Universe $t_0 = 19.0 \pm 0.7$ [Gyr] at 1σ CL. Ultimately, we obtained late-time accelerating power-law solutions supported

by the most recent cosmological data, and we proposed an alternative explanation for the origin of cosmic acceleration other than Λ CDM. Our results generalize and significantly improve previous achievements in the literature, highlighting the practical implications of fractional calculus in Cosmology.

Keywords: Fractional calculus; dynamical systems; scalar field cosmology; modified gravity.

1. INTRODUCTION

In Λ CDM cosmology, the dark energy component is represented by a cosmological constant (Λ), while cold dark matter (CDM) is also present. The Λ CDM model explains the observed late-time acceleration of the Universe suggested by Type Ia supernovae (SnIa) [1] and confirmed by Cosmic Microwave Background radiation [2]. Additionally, it accurately describes the formation of the Universe's structure according to observations. However, the model suffers from the well-known Cosmological Constant problem [3, 4], and the source of the late-time acceleration of the Universe has yet to be unveiled [5]. Some alternative theories to Λ CDM include noncommutative theories, quantum cosmology, quantum deformation, deformed phase space, Brans-Dicke theory, and noncommutative minisuperspace [6–12]. Phantom fields introduce “exotic physics” due to their negative kinetic energy and quantum instability, although supported by observations [13–16]. Quintom models are also introduced [17–40], and related Chiral generalized cosmology model in [41, 42]. The crossing of the phantom divide is also possible in the context of scalar-tensor theories [43–48] as well as in modified theories of gravity [49–74]. In [74], are investigated $F(R) = R^n$ theories in anisotropic Kantowski-Sachs (KS) metrics. In this scenario, the Universe, at late times, can produce accelerated expansion; additionally, it exhibits phantom behavior for a particular n range ($2 < n < 3$). For ($n = 2, w = 1/3$), the stable solution corresponds to a de Sitter

*Electronic address: bayron.micolta@alumnos.ucn.cl

†Electronic address: alfredo.millano@alumnos.ucn.cl

‡Electronic address: genly.leon@ucn.cl

§Electronic address: byron.droguett@uantof.cl

¶Electronic address: esteban.gonzalez@ucn.cl

**Electronic address: juan.magana@ucn.cl

expansion describing the inflationary epoch of the Universe. The Kantowski-Sachs anisotropic R^n -gravity can also lead to either accelerating or decelerating contracting solutions, but they are not globally stable. Thus, the Universe can remain near these saddles before approaching the expanding, accelerating, late-time attractors. In [75] was performed a detailed phase-space analysis of Hořava-Lifshitz cosmology, with and without the detailed-balance condition. Under detailed balance, the Universe can reach a bouncing oscillatory state at late times, in which dark energy, behaving as a simple cosmological constant, is dominant. Since the phase space of Hořava-Lifshitz is generally non-compact, by performing a Poincaré compactification process that allows for the construction of a global phase space containing all the cosmological information [75]. Recently, the nonprojectable Hořava version has been shown to be renormalizable [76, 77]. In [78], a dynamical system was devised to investigate the dynamics near the initial singularity, obtaining in that regime: radiation-dominated scaling solutions; power-law inflationary scalar field dominated solutions; matter-kinetic-radiation scaling solutions; matter-potential-radiation scaling solutions. In [79–81], a dynamical system was devised to describe the past asymptotic dynamics in coupled dark energy models, allowing scaling solutions to be classified. It was proved that the equilibrium points corresponding to the nonnegative local minimums of the potential (associated with cosmological de Sitter solutions) are asymptotically stable. In [82], varying-mass dark matter particles in phantom cosmology were studied.

Traditional mathematical models for integer-order derivatives often need to be modified when dealing with power law phenomena. In these cases, alternative modeling tools like fractional calculus should accurately capture power law behavior's non-local, frequency-dependent, and history-dependent properties. That involves extending the classical integer order calculus to include derivatives and integrals of arbitrary (real or complex) order. The study of fractional calculus is interdisciplinary in nature and has applications across various fields, making it a valuable area of research [83–91]. Recent studies have shown that fractional calculus is also helpful in modeling fractional derivatives and quantum fields [92, 93], quantum gravity and cosmology [94–99], black holes [100, 101], fractional dynamics and fractional action cosmology [102–109], non-minimal couplings [95, 110, 111], fractal universe and quantum cosmology [112, 113], multiscale gravity [114], classical and quantum gravity with fractional operators [115, 116], multi-fractional spacetimes [117], quantum gravity and gravitational-wave astronomy [118], cosmic microwave background and inflation [119],

fractional dynamics from Einstein gravity [100, 120], and fractional cosmology [110, 121–124] and dark energy, among others [125–132].

It is conceivable to develop fractional versions of Newtonian mechanics and Friedman-Robertson-Walker cosmology by substituting partial and fractional derivatives in familiar equations. In cosmology, the fractional order of differentiation (denoted by the symbol μ) could be a variable that changes with time, although this idea has yet to be thoroughly explored. The results derived from fractional derivatives are consistent with expectations, but initiating the process with fractional derivatives is essential for coherence. That brings us to the topic of fractional derivative geometry. It is necessary to clarify what fractional derivative geometry should entail. In [121], the authors initially attempted to envision the possible curvature and line elements in two dimensions. Fractional Lagrangian densities have become popular in addressing cosmological problems and obtaining modified models. For instance, a fractional theory of gravitation has been developed for fractional spacetime, resulting in new classes of cosmological models. Dynamical system methods, in combination with testing against observational data, provide a robust approach to investigating the physical behavior of cosmological models [133–136]. They can be used in new contexts, such as [130], where dynamical systems were used to analyze a fractional cosmology for different matter contents, obtaining a cosmology with late acceleration without including dark energy [127, 131, 132]. In reference [127], a joint analysis was performed using cosmic chronometers and type Ia supernovae data. This comparison with observational tests was used to find the best-fit values for the fractional order of the derivative. Based on the work presented in [127], two research paths were identified for the cosmological model without a scalar field. The first path compares with the standard model, assuming that the Universe's components are cold dark matter and radiation. The second path entails deducing the equation of state for one of the matter sources based on compatibility conditions [130], not previously analyzed in [127].

On the other hand, in Gauss-Bonnet (GB) theory, the Gauss-Bonnet scalar modifies the Einstein-Hilbert Action. The Gauss-Bonnet scalar is a topological invariant in four dimensions, making the theory equivalent to General Relativity [137]. However, the four-dimensional Einstein-scalar-Gauss-Bonnet theory has been previously introduced [138–144], where the scalar field interacts with the Gauss-Bonnet scalar through a non-constant function. The mass of the scalar field depends on the topological invariant of the Gauss-Bonnet scalar [145–148] which makes a non-zero contribution to the gravitational theory due to the coupling

functions between the Gauss-Bonnet scalar and the scalar field (as seen in [149, 150]). The authors examined different couplings and discovered that in four dimensions, equilibrium points describe zero acceleration and de Sitter solutions.

This paper presents a new theory, the Fractional Einstein-Gauss-Bonnet scalar field theory, with significant cosmological implications. Assuming the time conservation of the Friedmann equation (which is not granted as in General Relativity), we derive an evolution equation for an effective scalar field related to the coupling to the Gauss-Bonnet term. Our research reveals non-trivial solutions associated with exponential potential, exponential couplings to the Gauss-Bonnet term, and logarithmic scalar field, which depend on two cosmological parameters and the fractional derivative order μ . We obtain stability conditions for the exact solution by employing linear stability theory. We investigate the scaling behavior of the solutions and how the geometric corrections in the coupling to the Gauss-Bonnet scalar mimic the behavior of the dark sector in modified gravity. Using data from cosmic chronometers, type Ia supernovae, supermassive black hole shadows, and strong gravitational lensing, we estimate the values of the free parameters, indicating that the solution is consistent with the current observational constraints providing a late-time accelerating power-law solution for the scale factor. We also examine the physical interpretation of the cosmological solutions, focusing on the influence of the fractional order of the derivative in a theory of gravity that includes a scalar field minimally coupled to gravity and nonminimally coupled to the four-dimensional Gauss-Bonnet invariant.

In classical cosmology, fractional derivative methods have been established using two approaches. The first method, the last-step modification method, involves replacing the given cosmological field equations with fractional field equations for a specific model. An example of this method is explained in [151]. The second method, the first-step modification method, is a more fundamental approach. In this method, a fractional derivative geometry is first established, and then the variational principle for fractional action is applied to derive a modified cosmological model. This method involves defining the fractional derivative and establishing the variational principle to model the dynamic properties of fields [152–158]. Our manuscript is organized as follows.

In §2, we will use fractional differential calculus to calculate specific physical quantities. A critical application of these techniques is in cosmology. Instead of using covariant fractional derivatives to replace the usual covariant derivatives, we will utilize the point-like Lagrangian

formulation of cosmology in the flat FLRW metric and then extend such action to the fractional framework. Obtaining specific approximate values for cosmological quantities is unsurprising, assuming they can be defined. That is because the fractional modification of the concept of derivative can be manipulated to yield results that can be compared to cosmological measurements. Due to their interest in cosmology, §3 discusses scaling solutions and provides a reconstruction procedure for the potential and the coupling function. The stability analysis of the exact solution is performed in §4. In §5, we shall constrain the free parameters of the exact scaling solution obtained. For that end, we compute the best-fit parameters at 1σ (68.3%) of confidence level (CL) for the supernovae Ia (SNe Ia), cosmic chronometers (CC), gravitational lensing (GL), and black hole shadows (BHS) data. We conclude in §6. For completeness, in Appendix A, we present our variational equations, and in Appendix B, we present the formalism for the stability analysis of power-law solutions $\psi_s(t)$ of a generic ordinary differential equation $\mathcal{F}(t, \psi(t), \dot{\psi}(t), \ddot{\psi}(t), \dots) \equiv 0$ where $t > 0$ is the independent variable and $\psi(t)$ is the dependent variable using similar methods as in Ratra & Peebles, [159], Liddle & Scherrer [160] and Uzan [161].

2. EINSTEIN-GAUSS-BONNET SCALAR FIELD GRAVITY

In this section, we start with an action with a scalar field with a non-zero coupling to the Gauss-Bonnet term,

$$S = \int d^4x \sqrt{-g} \left[\frac{R}{2\kappa^2} - \frac{1}{2} g^{\mu\nu} \partial_\mu \phi \partial_\nu \phi - V(\phi) - f(\phi) \mathcal{G} \right], \quad (1)$$

where R is the Ricci scalar and we use units where $\kappa^2 = 8\pi G = 1$, and \mathcal{G} is the Gauss-Bonnet term:

$$\mathcal{G} = R^2 - 4R_{\alpha\beta}R^{\alpha\beta} + R_{\alpha\beta\gamma\delta}R^{\alpha\beta\gamma\delta}. \quad (2)$$

Here, ϕ is a scalar field minimally coupled to gravity with self-interacting potential $V(\phi)$, which is nonminimally coupled to the Gauss-Bonnet invariant \mathcal{G} through the coupling function $f(\phi)$. We are considering the Friedmann-Lemaître-Robertson-Walker metric

$$ds^2 = -N^2(t) dt^2 + a^2(t) (dx^2 + dy^2 + dz^2). \quad (3)$$

Defining $H = \dot{a}/(Na)$ we obtain that the Ricci scalar and the GB term are given by

$$R = 12H^2 + 6\dot{H}/N, \quad \mathcal{G} = 24H^2 \left(H^2 + \dot{H}/N \right). \quad (4)$$

By substituting R and \mathcal{G} into the action, we can find the point-like lagrangian:

$$\begin{aligned} \mathcal{L} = & \dot{N}(\theta) \left[\frac{24\dot{a}(\theta)^3 f(\phi(\theta))}{N(\theta)^4} - \frac{3a(\theta)^2 \dot{a}(\theta)}{N(\theta)^2} \right] + \frac{3a(\theta) \dot{a}(\theta)^2}{N(\theta)} \\ & + \ddot{a}(\theta) \left[\frac{3a(\theta)^2}{N(\theta)} - \frac{24\dot{a}(\theta)^2 f(\phi(\theta))}{N(\theta)^3} \right] + \frac{a(\theta)^3 \dot{\phi}(\theta)^2}{2N(\theta)} - a(\theta)^3 N(\theta) V(\phi(\theta)). \end{aligned} \quad (5)$$

Extending this model using fractional calculus, we consider that the action is defined by

$$S(\tau) = \frac{1}{\Gamma(\mu)} \int_0^\tau \mathcal{L}(\theta, q_i(\theta), \dot{q}_i(\theta), \ddot{q}_i(\theta)) (\tau - \theta)^{\mu-1} d\theta. \quad (6)$$

We follow the procedures of reference [162], which start with the action (6). We make the steps in appendix A to obtain the equations of motion of the fields. Implementing the derivatives in (A7), we have

$$\begin{aligned} & \frac{\partial \mathcal{L}(\theta, q_i(\theta), \dot{q}_i(\theta), \ddot{q}_i(\theta))}{\partial q_i} - \frac{d}{d\theta} \frac{\partial \mathcal{L}(\theta, q_i(\theta), \dot{q}_i(\theta), \ddot{q}_i(\theta))}{\partial \dot{q}_i} + \frac{d^2}{d\theta^2} \frac{\partial \mathcal{L}(\theta, q_i(\theta), \dot{q}_i(\theta), \ddot{q}_i(\theta))}{\partial \ddot{q}_i} \\ & = \frac{1 - \mu}{\tau - \theta} \left[\frac{\partial \mathcal{L}(\theta, q_i(\theta), \dot{q}_i(\theta), \ddot{q}_i(\theta))}{\partial \dot{q}_i} - 2 \frac{d}{d\theta} \frac{\partial \mathcal{L}(\theta, q_i(\theta), \dot{q}_i(\theta), \ddot{q}_i(\theta))}{\partial \ddot{q}_i} \right] \\ & - \frac{(1 - \mu)(2 - \mu)}{(\tau - \theta)^2} \frac{\partial \mathcal{L}(\theta, q_i(\theta), \dot{q}_i(\theta), \ddot{q}_i(\theta))}{\partial \ddot{q}_i}. \end{aligned} \quad (7)$$

Then, by applying Hamilton's principle, we obtain the Euler-Poisson equations modified by the fractional parameter μ given by (7) by taking the variations with respect to $q_i \in \{N, a, \phi\}$, and making $N = 1$ after the variation. Then, using the parameterization $(\tau, \theta) = (2t, t)$, we obtain respectively the Friedmann, Raychaudhuri and Klein-Gordon equations:

$$\begin{aligned} & \frac{24\dot{a}^3 \dot{\phi} f'(\phi)}{a^3} - \frac{24(\mu - 1)\dot{a}^3 f(\phi)}{ta^3} - \frac{3\dot{a}(t\dot{a} - \mu a + a)}{ta^2} + V(\phi) + \frac{1}{2} \dot{\phi}^2 = 0, \quad (8) \\ & - \frac{2\ddot{a}}{a} + \frac{8\dot{a}^2 \dot{\phi}^2 f''(\phi)}{a^2} + \frac{\dot{a}[2(\mu - 1)a - t\dot{a}]}{ta^2} + f'(\phi) \left[-\frac{16(\mu - 1)\dot{a}^2 \dot{\phi}}{ta^2} + \frac{8\dot{a}^2 \ddot{\phi}}{a^2} + \frac{16\dot{a}\ddot{a}\dot{\phi}}{a^2} \right] \end{aligned}$$

$$+ f(\phi) \left[\frac{8(\mu - 2)(\mu - 1)\dot{a}^2}{t^2 a^2} - \frac{16(\mu - 1)\dot{a}\ddot{a}}{ta^2} \right] - \frac{(\mu - 2)(\mu - 1)}{t^2} + V(\phi) - \frac{1}{2} \dot{\phi}^2 = 0, \quad (9)$$

$$- \frac{3\dot{a}\dot{\phi}}{a} - \frac{24\dot{a}^2 \ddot{a} f'(\phi)}{a^3} + \frac{(\mu - 1)\dot{\phi}}{t} - V'(\phi) - \ddot{\phi} = 0. \quad (10)$$

Substituting $H = \dot{a}/a$ (with $N \equiv 1$) in (8)-(10), we have

$$24H^3\dot{\phi}f'(\phi) - \frac{24(\mu-1)H^3f(\phi)}{t} + \frac{3(\mu-1)H}{t} - 3H^2 + V(\phi) + \frac{1}{2}\dot{\phi}^2 = 0, \quad (11)$$

$$8H^2\dot{\phi}^2f''(\phi) + f'(\phi) \left[16H\dot{H}\dot{\phi} + H^2 \left(8\ddot{\phi} - \frac{16(\mu-1)\dot{\phi}}{t} \right) + 16H^3\dot{\phi} \right] \\ + f(\phi) \left[-\frac{16(\mu-1)H\dot{H}}{t} + \frac{8(\mu-2)(\mu-1)H^2}{t^2} - \frac{16(\mu-1)H^3}{t} \right] \\ - 2\dot{H} + \frac{2(\mu-1)H}{t} - 3H^2 - \frac{(\mu-2)(\mu-1)}{t^2} + V(\phi) - \frac{1}{2}\dot{\phi}^2 = 0, \quad (12)$$

$$-24H^2\dot{H}f'(\phi) - 24H^4f'(\phi) + \frac{(-3tH + \mu - 1)\dot{\phi}}{t} - V'(\phi) - \ddot{\phi} = 0. \quad (13)$$

By solving the system (11), (12), (13) for $V(\phi)$, $\ddot{\phi}$ and \dot{H} , we obtain the following equations:

$$V(\phi) = \frac{(3-3\mu)H}{t} + 3H^2 + \frac{24(-1+\mu)f(\phi)H^3}{t} - 24H^3f'(\phi)\dot{\phi} - \frac{1}{2}\dot{\phi}^2, \quad (14)$$

$$\ddot{\phi} = \frac{\left\{ 12t(-1+\mu)H^3f'(\phi) + t \left[-tV'(\phi) + (-1+\mu)\dot{\phi} \right] + 288tH^5f'(\phi) \left[(1-\mu)f(\phi) + tf'(\phi)\dot{\phi} \right] \right. \\ \left. + 12H^2 \left[-2t(-1+\mu)f(\phi)\dot{\phi} + f'(\phi) \left(2-3\mu+\mu^2+3t^2\dot{\phi}^2 \right) \right] + H \left[-8(-1+\mu)f(\phi) \left(tV'(\phi) - (-1+\mu)\dot{\phi} \right) + t\dot{\phi} \left(-3t+8f'(\phi) \left(tV'(\phi) - (-1+\mu)\dot{\phi} \right) \right) \right] \right. \\ \left. - 24H^4f'(\phi) \left[4(-2+\mu)(-1+\mu)f(\phi) + t \left(t+4\dot{\phi} \left(-2(-1+\mu)f'(\phi) + t\dot{\phi}f''(\phi) \right) \right) \right] \right\}}{t \left[t+8H \left((-1+\mu)f(\phi) + tf'(\phi) \left(12H^3f'(\phi) - \dot{\phi} \right) \right) \right]}, \quad (15)$$

$$\dot{H} = - \left\{ \left[2-3\mu+\mu^2+t(-1+\mu)H + 192t^2H^6f'(\phi)^2 + t^2\dot{\phi}^2 + 8tH^3 \left((1-\mu)f(\phi) + 4tf'(\phi)\dot{\phi} \right) \right. \right. \\ \left. \left. - 8H^2 \left((-2+\mu)(-1+\mu)f(\phi) + t \left(f'(\phi) \left(-tV'(\phi) - (-1+\mu)\dot{\phi} \right) + t\dot{\phi}^2f''(\phi) \right) \right) \right] \right\} / \\ \left[2t \left(t+8H \left((-1+\mu)f(\phi) + tf'(\phi) \left(12H^3f'(\phi) - \dot{\phi} \right) \right) \right) \right]. \quad (16)$$

We now impose that the time derivative of Friedmann equation (11) is zero under the hypothesis that $\mu \neq 1$ (for $\mu = 1$ is trivial), that is,

$$\frac{d}{dt} \left[24H^3\dot{\phi}f'(\phi) - \frac{24(\mu-1)H^3f(\phi)}{t} + \frac{3(\mu-1)H}{t} - 3H^2 + V(\phi) + \frac{1}{2}\dot{\phi}^2 \right] = 0. \quad (17)$$

Computing the time derivative and replacing $V(\phi)$, $\ddot{\phi}$ and \dot{H} given by (14), (15) and (16) into (17), we obtain

$$\begin{aligned}
0 = & \left\{ 3(-2 + \mu)(-1 + \mu) + t^2 \dot{\phi}^2 - 4608tH^7 f'(\phi)^2 \left[-((-3 + \mu)f(\phi)) + tf'(\phi)\dot{\phi} \right] \right. \\
& + 48tH^3 \left[-((1 + \mu)f(\phi)) + 2tf'(\phi)\dot{\phi} \right] + tH \left[15 - 3\mu - 16(-1 + \mu)f(\phi)\dot{\phi}^2 + 16tf'(\phi)\dot{\phi}^3 \right] \\
& - 576tH^5 \left[-((-1 + \mu)f(\phi)^2) + (-3 + \mu)f'(\phi)^2 + 2tf(\phi)f'(\phi)\dot{\phi} \right] \\
& - 48H^4 \left[-4(-1 + \mu)(-8 + 3\mu)f(\phi)^2 - 4t^2 f'(\phi)^2 \dot{\phi}^2 \right. \\
& \left. + tf(\phi) \left(-t + 4f'(\phi) \left(tV'(\phi) + (-9 + 5\mu)\dot{\phi} \right) - 4t\dot{\phi}^2 f''(\phi) \right) \right] \\
& \left. - 6H^2 \left(4f(\phi) \left(10 - 14\mu + 4\mu^2 + t^2 \dot{\phi}^2 \right) + t \left(t - 4f'(\phi) \left(tV'(\phi) + (-7 + 3\mu)\dot{\phi} \right) + 4t\dot{\phi}^2 f''(\phi) \right) \right) \right\} / \\
& \left\{ 2t^2 \left(t + 8H \left((-1 + \mu)f(\phi) + tf'(\phi) \left(12H^3 f'(\phi) - \dot{\phi} \right) \right) \right) \right\}. \tag{18}
\end{aligned}$$

We introduce the auxiliary field

$$\psi = f(\phi), \tag{19}$$

and we calculate the successive derivatives using the chain rule:

$$\dot{\psi} = \frac{d}{dt} f(\phi) = f'(\phi)\dot{\phi}, \ddot{\psi} = f''(\phi)\dot{\phi}^2 + f'(\phi)\ddot{\phi} = f''(\phi)\dot{\phi}^2 + \frac{\dot{\psi}}{\dot{\phi}}\ddot{\phi}. \tag{20}$$

In this way, we obtain

$$f'(\phi) = \frac{\dot{\psi}}{\dot{\phi}}, f''(\phi) = \frac{1}{\dot{\phi}^2} \left(\ddot{\psi} - \frac{\dot{\psi}}{\dot{\phi}}\ddot{\phi} \right). \tag{21}$$

Replacing the expression (21) into (14), (15), (16), and (18), and solving the resulting system for, $\ddot{\phi}$, $\ddot{\psi}$, \dot{H} and $V(\phi)$, it turns out

$$\ddot{\phi} = \frac{\frac{24(\mu-3)H^3\dot{\psi}}{\dot{\phi}} + (\mu-1)\dot{\phi}}{t} + \frac{192H^5\dot{\psi}^2}{(1-8H^2\psi)\dot{\phi}} + \dot{\phi} \left(\frac{8H^2\dot{\psi}}{1-8H^2\psi} - 3H \right) - V'(\phi), \quad (22)$$

$$\begin{aligned} \ddot{\psi} = & \frac{(\mu-1) \left[\frac{\mu-2}{H^2} + 8(8-3\mu)\psi \right]}{8t^2} \\ & + \frac{2\dot{\psi} \left(\frac{\mu-1}{8H^2\psi-1} + 3\mu - 5 \right) - 3(\mu-1)H\psi + \frac{2(\mu-1)\psi\dot{\phi}^2}{3H(8H^2\psi-1)} - \frac{\mu-5}{8H}}{t} \\ & + \frac{16H^2\dot{\psi}^2}{1-8H^2\psi} + H \left(\frac{2}{8H^2\psi-1} + 3 \right) \dot{\psi} + \dot{\phi}^2 \left(\frac{2\dot{\psi}}{3H-24H^3\psi} + \frac{\frac{2}{8H^2\psi-1} + 3}{24H^2} \right) - \frac{1}{4}, \end{aligned} \quad (23)$$

$$\dot{H} = -\frac{(\mu-3)H}{t} + \frac{8H^3\dot{\psi}}{8H^2\psi-1} + \frac{\dot{\phi}^2}{24H^2\psi-3} - H^2, \quad (24)$$

$$V(\phi) = \frac{3(\mu-1)H(8H^2\psi-1)}{t} - 24H^3\dot{\psi} + 3H^2 - \frac{1}{2}\dot{\phi}^2. \quad (25)$$

From equation (25), we define the effective energy densities

$$\rho_\phi = \frac{1}{2}\dot{\phi}^2 + V(\phi), \rho_{\text{fracc}} = \frac{3(\mu-1)}{t}H, \rho_{\text{GB}} = 24H^3\dot{\psi}, \rho_{\text{GB, fracc}} = -\frac{24(\mu-1)}{t}H^3\psi, \quad (26)$$

such that (11) is reduced to

$$3H^2 = \rho_\phi + \rho_{\text{fracc}} + \rho_{\text{GB}} + \rho_{\text{GB, fracc}}. \quad (27)$$

3. EXACT SCALING SOLUTIONS

We can find an analytical solution to the system by considering

$$H = \frac{2}{m}t^{-p}, \quad (28)$$

$$\psi = F_0t^q, \quad (29)$$

$$\phi = \frac{2\ln(t)}{\lambda}, \quad \lambda \neq 0, \quad (30)$$

where m , F_0 , p , q and λ are constants.

Then, the equations (22), (23), (24) and (25) are written

$$\begin{aligned} & \frac{64F_0(q-\mu)t^q + 2\mu m^2 t^{2p}}{\lambda t^2 (m^2 t^{2p} - 32F_0 t^q)} - \frac{96F_0 \lambda q(-\mu + q + 3)t^{q-3p-1}}{m^3} + \frac{3\lambda m q^2 t^{p-1}}{m^2 t^{2p} - 32F_0 t^q} \\ & - \frac{3t^{-p-1}(\lambda^2 q^2 + 4)}{\lambda m} - V'(\ln(t^{2/\lambda})) = 0, \end{aligned} \quad (31)$$

$$\begin{aligned} & \frac{m^4 [3\lambda^2(\mu-2)(\mu-1) + 4] t^{4p-2}}{96\lambda^2 (m^2 t^{2p} - 32F_0 t^q)} - \frac{1}{4} \\ & + \frac{32F_0^2 [-11\mu + 3(\mu^2 - 2\mu q + q(q+3)) + 8] t^{2q-2}}{m^2 t^{2p} - 32F_0 t^q} \\ & - \frac{F_0 m^2 t^{2p+q-2} [\lambda^2(-2\mu + q + 2)(-2\mu + q + 5) + 4]}{\lambda^2 (m^2 t^{2p} - 32F_0 t^q)} + \frac{4F_0 m^3 (-\mu + q + 1)t^{3p+q-3}}{3\lambda^2 (m^2 t^{2p} - 32F_0 t^q)} \\ & + \frac{1}{16} m t^{p-1} \left(-\frac{64F_0 q t^q}{m^2 t^{2p} - 32F_0 t^q} - \mu + 5 \right) + \frac{6F_0(-\mu + q + 1)t^{q-p-1}}{m} = 0, \end{aligned} \quad (32)$$

$$\frac{4}{3\lambda^2 t^2 \left(\frac{32F_0 t^{q-2p}}{m^2} - 1 \right)} + \frac{2t^{-p-1}(-\mu + p + q + 3)}{m} - \frac{2m q t^{p-1}}{m^2 t^{2p} - 32F_0 t^q} - \frac{4t^{-2p}}{m^2} = 0, \quad (33)$$

$$\frac{6t^{-3p-1} [32F_0(\mu - q - 1)t^q - (\mu - 1)m^2 t^{2p}]}{m^3} + \frac{12t^{-2p}}{m^2} - V(\ln(t^{2/\lambda})) - \frac{2}{\lambda^2 t^2} = 0. \quad (34)$$

Comparing the coefficients of t in the last equation, we have, by dimensional analysis, that

$$q = 2p, -2p = -2 \implies p = 1, q = 2. \quad (35)$$

For $p = 1$ and $q = 2$ and assuming $m^2 - 32F_0 \neq 0$, $m \neq 0$ and $\lambda \neq 0$ we have

$$\begin{aligned} & 6144F_0^2 \lambda^2 (\mu - 5) + 64F_0 m^2 [-3\lambda^2 (\mu - 3) + (\mu - 2)m - 6] \\ & + \lambda m^3 t^2 (m^2 - 32F_0) V'(\ln(t^{2/\lambda})) - 2m^4 (\mu m - 6) = 0, \end{aligned} \quad (36)$$

$$\begin{aligned} & 3072F_0^2 \lambda^2 [6(\mu - 3) + (\mu(3\mu - 23) + 38)m] \\ & - 64F_0 m [-12\lambda^2 + 2(\mu - 3)m^3 + m^2 (3\lambda^2 (\mu - 2)(2\mu - 7) + 6) + 6\lambda^2 \mu m] \\ & + m^3 [-24\lambda^2 + m^2 (3\lambda^2 (\mu - 2)(\mu - 1) + 4) - 6\lambda^2 (\mu - 5)m] = 0, \end{aligned} \quad (37)$$

$$192F_0 \lambda^2 + 96F_0 \lambda^2 (\mu - 6)m - 2m^4 - 3\lambda^2 (\mu - 4)m^3 - 6\lambda^2 m^2 = 0, \quad (38)$$

$$\frac{2[-96F_0 \lambda^2 (\mu - 3) + m^3 + 3\lambda^2 (\mu - 1)m^2 - 6\lambda^2 m]}{\lambda^2 m^3 t^2} - V(\ln(t^{2/\lambda})) = 0. \quad (39)$$

The last equation (39) allows us to reconstruct the Gauss-Bonnet coupling and scalar field potentials, which replicate scaling behaviors.

In our scenario, say, we acquire the exponential potential

$$V(\phi) = \frac{2e^{-\lambda\phi} [96F_0 \lambda^2 (\mu - 3) - m^3 - 3\lambda^2 (\mu - 1)m^2 + 6\lambda^2 m]}{\lambda^2 m^3}. \quad (40)$$

Replacing the derivative of potential (40) in equation (36), and assuming $(\mu - 6)m + 2 \neq 0$ and $m \neq 0$, results two independent equations:

$$F_0 = \frac{1}{96}m^2 \left[\frac{2m(3\lambda^2 + m)}{\lambda^2((\mu - 6)m + 2)} + 3 \right], \quad (41)$$

$$0 = (3\lambda^2 + m) [m(3\lambda^2(\mu + 2) - 4\mu + ((\mu - 5)\mu + 2)m + 30) - 6(3\lambda^2 + 2)]. \quad (42)$$

The first condition is the definition of F_0 . Hence, we have the two-parametric family of solutions (recall $\lambda = \lambda(m, \mu)$),

$$R(t) = -\frac{12(m-4)}{m^2t^2} \xrightarrow[\text{Using (30)}]{\implies} R(\phi) = -\frac{12(m-4)e^{-\lambda\phi}}{m^2}, \quad (43)$$

$$\mathcal{G}(t) = -\frac{192(m-2)}{m^4t^4} \implies \mathcal{G}(\phi) = -\frac{192(m-2)e^{-2\lambda\phi}}{m^4}, \quad (44)$$

$$H(t) = \frac{2}{mt} \implies H(\phi) = \frac{2}{m}e^{-\frac{\lambda\phi}{2}}, \quad (45)$$

$$\begin{aligned} \psi(t) &= \frac{1}{96}m^2t^2 \left[\frac{2m(3\lambda^2 + m)}{\lambda^2[(\mu - 6)m + 2]} + 3 \right] \\ &\implies f(\phi) = \frac{1}{96}m^2e^{\lambda\phi} \left[\frac{2m(3\lambda^2 + m)}{\lambda^2[(\mu - 6)m + 2]} + 3 \right], \end{aligned} \quad (46)$$

$$V(t) = \frac{2[12\lambda^2 + \mu m^3 + 2(9\lambda^2 - 1)m^2 + 6\lambda^2(\mu - 8)m]}{\lambda^2m^2t^2[(\mu - 6)m + 2]} \quad (47)$$

$$\implies V(\phi) = \frac{2e^{-\lambda\phi}[12\lambda^2 + \mu m^3 + 2(9\lambda^2 - 1)m^2 + 6\lambda^2(\mu - 8)m]}{\lambda^2m^2[(\mu - 6)m + 2]}. \quad (48)$$

Replacing the derivative of potential (40) in equation (36), we obtain the conditions on the parameters

$$\begin{aligned} 6144F_0^2\lambda^2(\mu - 4) + 32F_0m[6\lambda^2 + m(3\lambda^2(7 - 3\mu) + (\mu - 3)m - 6)] \\ + m^3[m(3\lambda^2(\mu - 1) - \mu m + m + 6) - 6\lambda^2] = 0, \end{aligned} \quad (49)$$

together with (37) and (38). Reducing the conditions and assuming $(\mu - 6)m + 2 \neq 0$ and $m \neq 0$, we obtain the cases:

1. For $0 < \mu \leq \frac{1}{2}(5 - \sqrt{17})$ and $\frac{2\mu-15}{\mu^2-5\mu+2} + \sqrt{\frac{16\mu^2-120\mu+249}{(\mu^2-5\mu+2)^2}} < m < \frac{6}{\mu+2}$,
 $\lambda = \frac{1}{3}\sqrt{\frac{36-3m[-4\mu+((\mu-5)\mu+2)m+30]}{(\mu+2)m-6}}$ and $F_0 = \frac{m^2(m(-4\mu+((\mu-2)(\mu-1)m+18)-12))}{32(m(-4\mu+((\mu-5)\mu+2)m+30)-12)}$. For $\mu = \frac{1}{2}(5 - \sqrt{17})$ and $\frac{1}{83}(60 - 6\sqrt{17}) < m < \frac{1}{16}(27 + 3\sqrt{17})$, $\lambda = \frac{2}{3}\sqrt{\frac{3(10+\sqrt{17})m-18}{(\sqrt{17}-9)m+12}}$ and $F_0 = -\frac{m^2((\sqrt{17}-5)m^2-2(4+\sqrt{17})m+12)}{64((10+\sqrt{17})m-6)}$.

2. For $\frac{1}{2}(5 - \sqrt{17}) < \mu \leq 4$ and $m > \frac{2\mu-15}{\mu^2-5\mu+2} - \sqrt{\frac{16\mu^2-120\mu+249}{(\mu^2-5\mu+2)^2}}$ we have
 $\lambda = \frac{\sqrt{36-3m[-4\mu+((\mu-5)\mu+2)m+30]}}{3\sqrt{(\mu+2)m-6}}$ and $F_0 = \frac{m^2(m(-4\mu+(\mu-2)(\mu-1)m+18)-12)}{32(m(-4\mu+((\mu-5)\mu+2)m+30)-12)}$.
3. For $4 < \mu \leq \frac{1}{2}(5 + \sqrt{17})$ and $\frac{6}{\mu+2} < m < \frac{2\mu-15}{\mu^2-5\mu+2} + \sqrt{\frac{16\mu^2-120\mu+249}{(\mu^2-5\mu+2)^2}}$ we have
 $\lambda = \frac{\sqrt{36-3m[-4\mu+((\mu-5)\mu+2)m+30]}}{3\sqrt{(\mu+2)m-6}}$ and $F_0 = \frac{m^2(m(-4\mu+(\mu-2)(\mu-1)m+18)-12)}{32(m(-4\mu+((\mu-5)\mu+2)m+30)-12)}$. For $\mu = \frac{1}{2}(5 + \sqrt{17})$ and $\frac{1}{16}(27 - 3\sqrt{17}) < m < \frac{1}{83}(60 + 6\sqrt{17})$ we have
 $\lambda = 2\sqrt{\frac{(\sqrt{17}-10)m+6}{3(9+\sqrt{17})m-36}}$ and $F_0 = \frac{m^2(12-m((5+\sqrt{17})m-2\sqrt{17}+8))}{64((\sqrt{17}-10)m+6)}$.
4. For $4 < \mu < \frac{1}{2}(5 + \sqrt{17})$ and $m > \frac{2\mu-15}{\mu^2-5\mu+2} - \sqrt{\frac{16\mu^2-120\mu+249}{(\mu^2-5\mu+2)^2}}$ we have
 $\lambda = \frac{\sqrt{36-3m[-4\mu+((\mu-5)\mu+2)m+30]}}{3\sqrt{(\mu+2)m-6}}$ and $F_0 = \frac{m^2(m(-4\mu+(\mu-2)(\mu-1)m+18)-12)}{32(m(-4\mu+((\mu-5)\mu+2)m+30)-12)}$.
5. For $\mu > \frac{1}{2}(5 + \sqrt{17})$ and $\frac{6}{\mu+2} < m < \frac{2\mu-15}{\mu^2-5\mu+2} + \sqrt{\frac{16\mu^2-120\mu+249}{(\mu^2-5\mu+2)^2}}$ we have $\lambda = \frac{1}{3}\sqrt{\frac{36-3m[-4\mu+((\mu-5)\mu+2)m+30]}{(\mu+2)m-6}}$ and $F_0 = \frac{m^2(m(-4\mu+(\mu-2)(\mu-1)m+18)-12)}{32(m(-4\mu+((\mu-5)\mu+2)m+30)-12)}$.

The allowed regions for the parameters μ and m are shown in Figure 1.

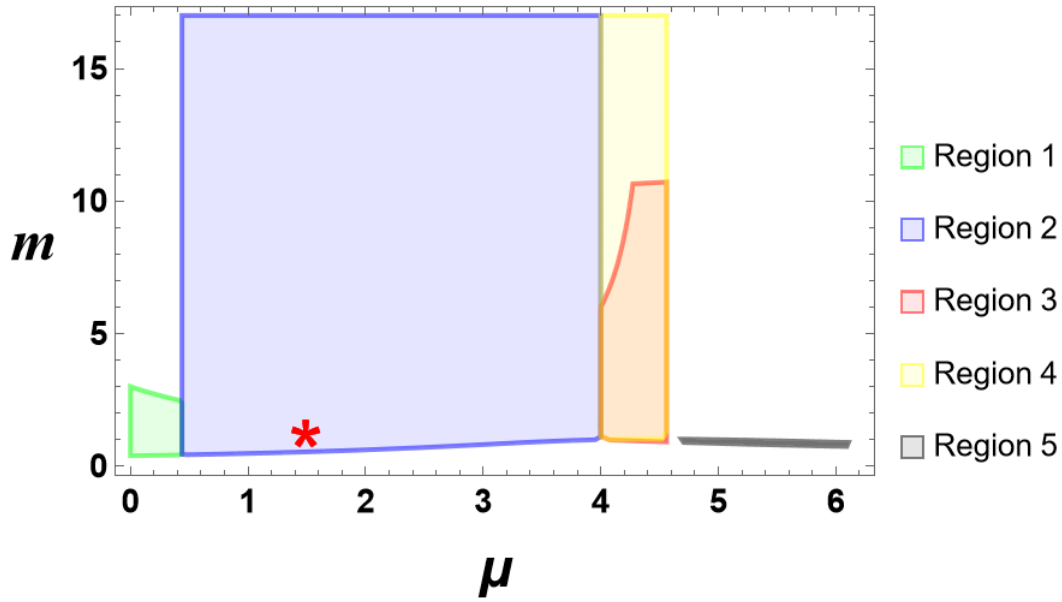


FIG. 1: Allowed regions for the parameters μ and m . The red star represents the point in the parameter space with the best-fit values of μ and m according to the analysis in §5.

Replacing the ansatz

$$H = \frac{2}{mt}, m \neq \frac{6}{\mu} \quad (50)$$

in the equations (22), (23), (24) and (25), we obtain

$$\ddot{\phi} = -\frac{6(m-2)[(\mu-4)m+2](m^2t^2-32\psi)}{m^5t^5\dot{\phi}} + \frac{[(\mu-2)m-4]\dot{\phi}}{mt} - V'(\phi(t)), \quad (51)$$

$$\begin{aligned} \ddot{\psi} &= \frac{[m(\mu((\mu-7)m+4)-6)+4]\psi}{m^2t^2} \\ &+ \frac{1}{96} \left[m^2t^2(2-\mu m)\dot{\phi}^2 + 3m(-4\mu + (2-(\mu-5)\mu)m+2) - 12 \right], \end{aligned} \quad (52)$$

$$\dot{\psi} = \frac{[(\mu-4)m+2]\psi}{mt} - \frac{1}{192}mt \left[m^2t^2\dot{\phi}^2 + 6(\mu-4)m+12 \right], \quad (53)$$

$$V(\phi) = \frac{6(4-3m)m^2t^2 + 192(3m-2)\psi}{m^4t^4} + \frac{1}{2}\dot{\phi}^2. \quad (54)$$

To investigate the stability of the solution (45), (46), (30) and (47), we specify the potential (48), obtaining the equations

$$\begin{aligned} \ddot{\phi} &= \frac{192\lambda(3m-2)\psi}{m^4t^4} + \frac{6\lambda(4-3m)}{m^2t^2} + \frac{192(m-2)[(\mu-4)m+2]\psi}{m^5t^5} - \frac{6(m-2)[(\mu-4)m+2]}{m^3t^3} \\ &+ \frac{[(\mu-2)m-4]\dot{\phi}}{mt} + \frac{1}{2}\lambda\dot{\phi}^2, \end{aligned} \quad (55)$$

$$\begin{aligned} \ddot{\psi} &= \frac{[m(\mu((\mu-7)m+4)-6)+4]\psi}{m^2t^2} \\ &+ \frac{1}{96} \left[m^2t^2(2-\mu m)\dot{\phi}^2 + 3m(-4\mu + (2-(\mu-5)\mu)m+2) - 12 \right], \end{aligned} \quad (56)$$

$$\dot{\psi} = \frac{[(\mu-4)m+2]\psi}{mt} - \frac{1}{192}mt \left[m^2t^2\dot{\phi}^2 + 6(\mu-4)m+12 \right]. \quad (57)$$

After reducing the quadratic term $\dot{\phi}^2/2$ using the last equation, we obtain

$$\begin{aligned} \ddot{\phi} &= -\frac{96\lambda\dot{\psi}}{m^3t^3} - \frac{6(m-2)[(\mu-4)m+2]}{m^3t^3\dot{\phi}} - \frac{3\lambda[(\mu+2)m-6]}{m^2t^2} \\ &+ \psi \left[\frac{192(m-2)[(\mu-4)m+2]}{m^5t^5\dot{\phi}} + \frac{96\lambda[(\mu+2)m-2]}{m^4t^4} \right] + \frac{[(\mu-2)m-4]\dot{\phi}}{mt}, \end{aligned} \quad (58)$$

$$\begin{aligned} \ddot{\psi} &= \frac{1}{32} [m(-4\mu + (\mu-2)(\mu-1)m+18) - 12] \\ &+ \frac{[m(\mu(-\mu m + m+4) - 22) + 12]\psi}{m^2t^2} + \frac{2(\mu - \frac{2}{m})\dot{\psi}}{t}, \end{aligned} \quad (59)$$

$$\dot{\phi}^2 = \frac{192[(\mu-4)m+2]\psi}{m^4t^4} - \frac{192\dot{\psi}}{m^3t^3} - \frac{6[(\mu-4)m+2]}{m^2t^2}. \quad (60)$$

Equation (60) defines $\dot{\phi}$, and we analyze (59), our equation of interest. The general solution of (59) is

$$\begin{aligned} \psi(t) &= \frac{m^2t^2 [m(-4\mu + (\mu-2)(\mu-1)m+18) - 12]}{32 [m(-4\mu + ((\mu-5)\mu+2)m+30) - 12]} \\ &+ c_1 t^{\frac{2\mu m+m-4-\sqrt{m(8\mu m+m-96)+64}}{2m}} + c_2 t^{\frac{2\mu m+m-4+\sqrt{m(8\mu m+m-96)+64}}{2m}}. \end{aligned} \quad (61)$$

Taking $\psi(t)$ from (61), calculating its time derivative, $\dot{\psi}(t)$, and substituting in (60), $\phi(t)$ is given through the quadrature

$$\phi(t) = \pm \int_1^t \frac{\sqrt{-6[m(\mu-4)+2][m^2\eta^2-32\psi(\eta)]-192m\eta\psi'(\eta)}}{m^2\eta^2} d\eta + c_3. \quad (62)$$

4. STABILITY ANALYSIS OF THE EXACT SOLUTION

Denoting

$$\psi_c(t) = \frac{1}{96}m^2t^2 \left(\frac{2m(3\lambda^2+m)}{\lambda^2[(\mu-6)m+2]} + 3 \right), \quad (63)$$

$$\phi_c(t) = \frac{2\ln(t)}{\lambda}. \quad (64)$$

In this case, the evolution equation for ψ is decoupled.

Specializing the procedure in appendix B to the system (60)-(59), we define

$$\varepsilon(\tau) = \frac{\psi(\tau)}{\psi_c(\tau)} - 1. \quad (65)$$

Hence,

$$\ddot{\psi}(t) = \frac{m^2e^{2\tau}[6\lambda^2+2m^2+3\lambda^2(\mu-4)m][\varepsilon''(\tau)+3\varepsilon'(\tau)+2\varepsilon(\tau)+2]}{96\lambda^2t^2[(\mu-6)m+2]}, \quad (66)$$

$$\dot{\psi}(t) = \frac{m^2e^{2\tau}[6\lambda^2+2m^2+3\lambda^2(\mu-4)m][\varepsilon'(\tau)+2\varepsilon(\tau)+2]}{96\lambda^2t[(\mu-6)m+2]}, \quad (67)$$

$$\psi(t) = \frac{m^2e^{2\tau}[\varepsilon(\tau)+1][6\lambda^2+2m^2+3\lambda^2(\mu-4)m]}{96\lambda^2[(\mu-6)m+2]}. \quad (68)$$

Combining with equation (59) we obtain

$$\begin{aligned} \varepsilon''(\tau) &= \frac{36\lambda^2 - 2m[3\lambda^2(\mu+2) - 4\mu + ((\mu-5)\mu+2)m + 30] + 24}{\underbrace{6\lambda^2 + 2m^2 + 3\lambda^2(\mu-4)m}_{=0 \text{ by (42)}}} \\ &+ \frac{[12 - m(-4\mu + ((\mu-5)\mu+2)m + 30)]}{m^2} \varepsilon(\tau) + \left(2\mu - \frac{4}{m} - 3\right) \varepsilon'(\tau), \end{aligned} \quad (69)$$

where using the relation (42), the first term is zero. Defining $v(\tau) = \varepsilon'(\tau)$, we obtain the linear dynamical system

$$\varepsilon' = v, \quad (70)$$

$$v' = \frac{[12 - m(-4\mu + ((\mu-5)\mu+2)m + 30)]}{m^2} \varepsilon + \left(2\mu - \frac{4}{m} - 3\right) v. \quad (71)$$

4.1. Stability of the scaling solution

The scaling solution corresponds to the fixed point $(\varepsilon, v) = (0, 0)$. The matrix of the linear system is defined by

$$J(\varepsilon, v) = \begin{pmatrix} 0 & 1 \\ \frac{12-m[-4\mu+((\mu-5)\mu+2)m+30]}{m^2} & 2\mu - \frac{4}{m} - 3 \end{pmatrix}. \quad (72)$$

Evaluating the linear matrix around the fixed point, $\varepsilon = 0, v = 0$, we obtain the eigenvalues

$$\lambda_{1,2} = \frac{1}{2} \left(2\mu - \frac{4}{m} - 3 \pm \sqrt{\frac{m(8\mu m + m - 96) + 64}{m^2}} \right). \quad (73)$$

The origin is a sink for

1. $0 < \mu < \frac{1}{2} (5 - \sqrt{17})$, $\frac{2\mu-15}{\mu^2-5\mu+2} + \sqrt{\frac{16\mu^2-120\mu+249}{(\mu^2-5\mu+2)^2}} < m \leq \frac{48}{8\mu+1} - 8\sqrt{-\frac{8\mu-35}{(8\mu+1)^2}}$, or
2. $0 < \mu < \frac{1}{2} (5 - \sqrt{17})$, $m \geq 8\sqrt{-\frac{8\mu-35}{(8\mu+1)^2}} + \frac{48}{8\mu+1}$, or
3. $\mu = \frac{1}{2} (5 - \sqrt{17})$, $-\frac{6}{-10-\sqrt{17}} < m \leq \frac{48}{1+4(5-\sqrt{17})} - \frac{8\sqrt{35-4(5-\sqrt{17})}}{1+4(5-\sqrt{17})}$, or
4. $\mu = \frac{1}{2} (5 - \sqrt{17})$, $m \geq \frac{48}{1+4(5-\sqrt{17})} + \frac{8\sqrt{35-4(5-\sqrt{17})}}{1+4(5-\sqrt{17})}$, or
5. $\frac{1}{2} (5 - \sqrt{17}) < \mu < \frac{287+146\sqrt{3}}{148+80\sqrt{3}}$, $\frac{2\mu-15}{\mu^2-5\mu+2} - \sqrt{\frac{16\mu^2-120\mu+249}{(\mu^2-5\mu+2)^2}} < m \leq \frac{48}{8\mu+1} - 8\sqrt{-\frac{8\mu-35}{(8\mu+1)^2}}$, or
6. $\frac{1}{2} (5 - \sqrt{17}) < \mu < \frac{287+146\sqrt{3}}{148+80\sqrt{3}}$, $8\sqrt{-\frac{8\mu-35}{(8\mu+1)^2}} + \frac{48}{8\mu+1} \leq m < \frac{2\mu-15}{\mu^2-5\mu+2} + \sqrt{\frac{16\mu^2-120\mu+249}{(\mu^2-5\mu+2)^2}}$, or
7. $\frac{287+146\sqrt{3}}{148+80\sqrt{3}} \leq \mu < \frac{146\sqrt{3}-287}{80\sqrt{3}-148}$, $\frac{2\mu-15}{\mu^2-5\mu+2} - \sqrt{\frac{16\mu^2-120\mu+249}{(\mu^2-5\mu+2)^2}} < m \leq \frac{48}{8\mu+1} - 8\sqrt{-\frac{8\mu-35}{(8\mu+1)^2}}$.

The origin is a source for

1. $\frac{287+146\sqrt{3}}{148+80\sqrt{3}} < \mu \leq \frac{146\sqrt{3}-287}{80\sqrt{3}-148}$, $8\sqrt{-\frac{8\mu-35}{(8\mu+1)^2}} + \frac{48}{8\mu+1} \leq m < \frac{2\mu-15}{\mu^2-5\mu+2} + \sqrt{\frac{16\mu^2-120\mu+249}{(\mu^2-5\mu+2)^2}}$, or
2. $\frac{146\sqrt{3}-287}{80\sqrt{3}-148} < \mu < \frac{35}{8}$, $\frac{2\mu-15}{\mu^2-5\mu+2} - \sqrt{\frac{16\mu^2-120\mu+249}{(\mu^2-5\mu+2)^2}} < m \leq \frac{48}{8\mu+1} - 8\sqrt{-\frac{8\mu-35}{(8\mu+1)^2}}$, or
3. $\frac{146\sqrt{3}-287}{80\sqrt{3}-148} < \mu < \frac{35}{8}$, $8\sqrt{-\frac{8\mu-35}{(8\mu+1)^2}} + \frac{48}{8\mu+1} \leq m < \frac{2\mu-15}{\mu^2-5\mu+2} + \sqrt{\frac{16\mu^2-120\mu+249}{(\mu^2-5\mu+2)^2}}$, or
4. $\frac{35}{8} \leq \mu < \frac{1}{2} (5 + \sqrt{17})$, $\frac{2\mu-15}{\mu^2-5\mu+2} - \sqrt{\frac{16\mu^2-120\mu+249}{(\mu^2-5\mu+2)^2}} < m < \frac{2\mu-15}{\mu^2-5\mu+2} + \sqrt{\frac{16\mu^2-120\mu+249}{(\mu^2-5\mu+2)^2}}$, or
5. $\mu = \frac{1}{2} (5 + \sqrt{17})$, $m > -\frac{6}{\sqrt{17}-10}$, or

$$6. \mu > \frac{1}{2} (5 + \sqrt{17}), m > \frac{2\mu-15}{\mu^2-5\mu+2} + \sqrt{\frac{16\mu^2-120\mu+249}{(\mu^2-5\mu+2)^2}}.$$

The origin is a saddle for

$$1. 0 < \mu < \frac{1}{2} (5 - \sqrt{17}), 0 < m < \frac{2\mu-15}{\mu^2-5\mu+2} + \sqrt{\frac{16\mu^2-120\mu+249}{(\mu^2-5\mu+2)^2}}, \text{ OR}$$

$$2. \mu = \frac{1}{2} (5 - \sqrt{17}), 0 < m < -\frac{6}{-10-\sqrt{17}}, \text{ OR}$$

$$3. \frac{1}{2} (5 - \sqrt{17}) < \mu < \frac{1}{2} (5 + \sqrt{17}), 0 < m < \frac{2\mu-15}{\mu^2-5\mu+2} - \sqrt{\frac{16\mu^2-120\mu+249}{(\mu^2-5\mu+2)^2}}, \text{ OR}$$

$$4. \frac{1}{2} (5 - \sqrt{17}) < \mu < \frac{1}{2} (5 + \sqrt{17}), m > \frac{2\mu-15}{\mu^2-5\mu+2} + \sqrt{\frac{16\mu^2-120\mu+249}{(\mu^2-5\mu+2)^2}}$$

$$5. \mu = \frac{1}{2} (5 + \sqrt{17}), 0 < m < -\frac{6}{\sqrt{17}-10}, \text{ OR}$$

$$6. \mu > \frac{1}{2} (5 + \sqrt{17}), 0 < m < \frac{2\mu-15}{\mu^2-5\mu+2} + \sqrt{\frac{16\mu^2-120\mu+249}{(\mu^2-5\mu+2)^2}}.$$

Figure 2 shows the allowed regions by the parameters μ and m for the sink, source, and saddle cases. The red star represents the point in the parameter space with the best-fit values of μ and m according to the analysis in §5.

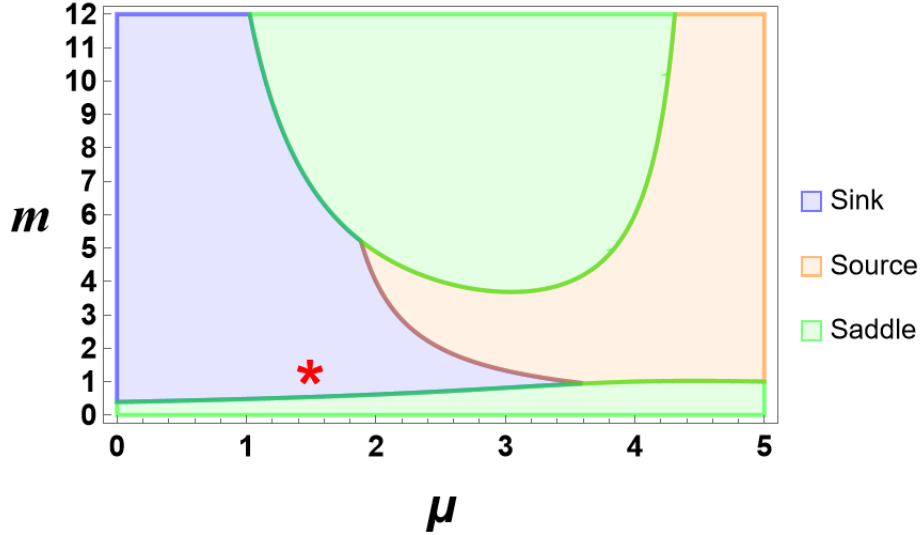


FIG. 2: Allowed regions by the parameters μ and m , for the sink, source, and saddle cases. The red star represents the point in the parameter space with the best-fit values of μ and m according to the analysis in §5.

Now we will show the flow of system (70)-(71). In Figure 3, we show some phase space diagrams for sink cases, in Figure 4 the source cases, and in Figure 5, the saddle cases.

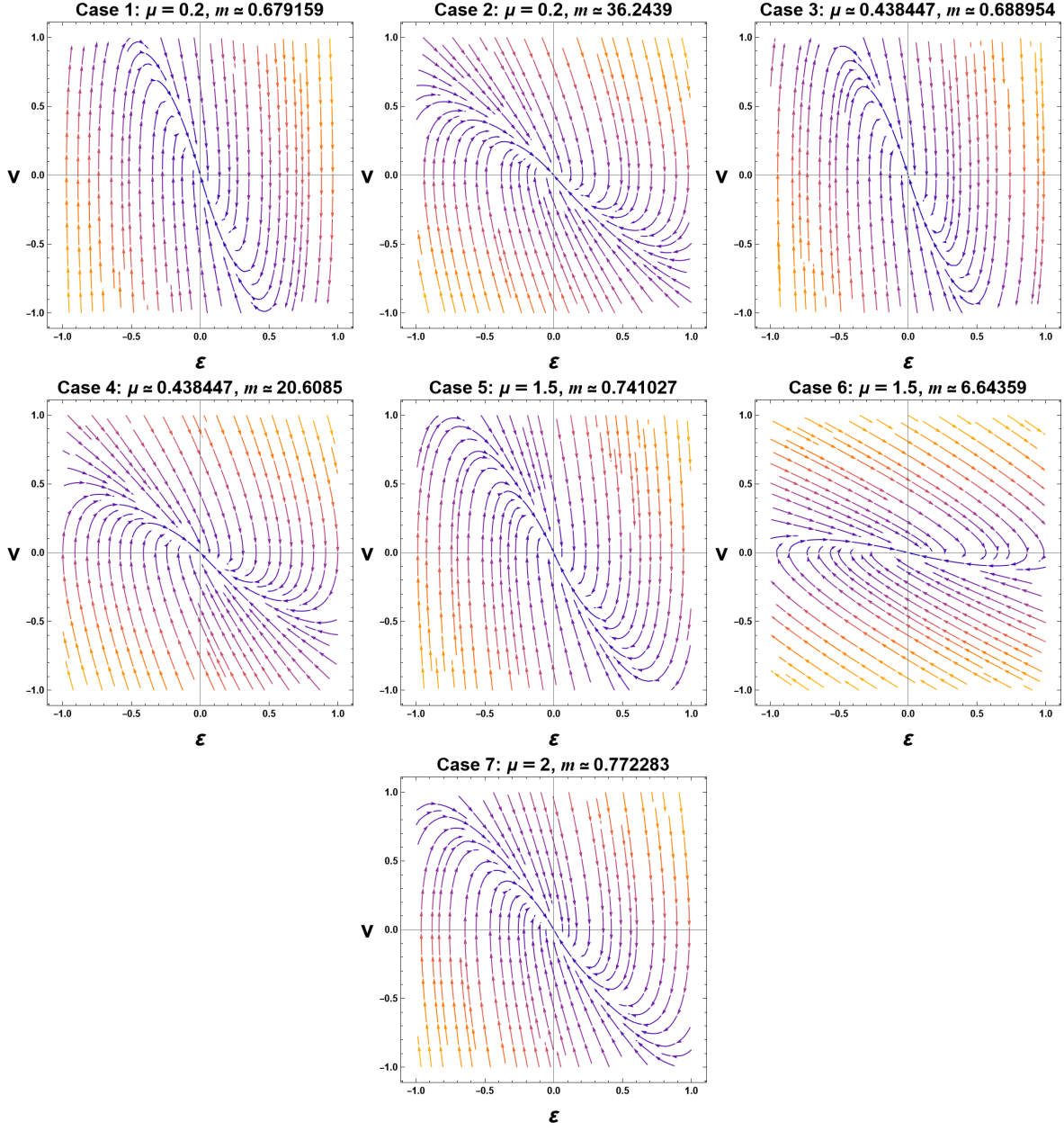


FIG. 3: Flow of system (70)-(71) for the sink cases.

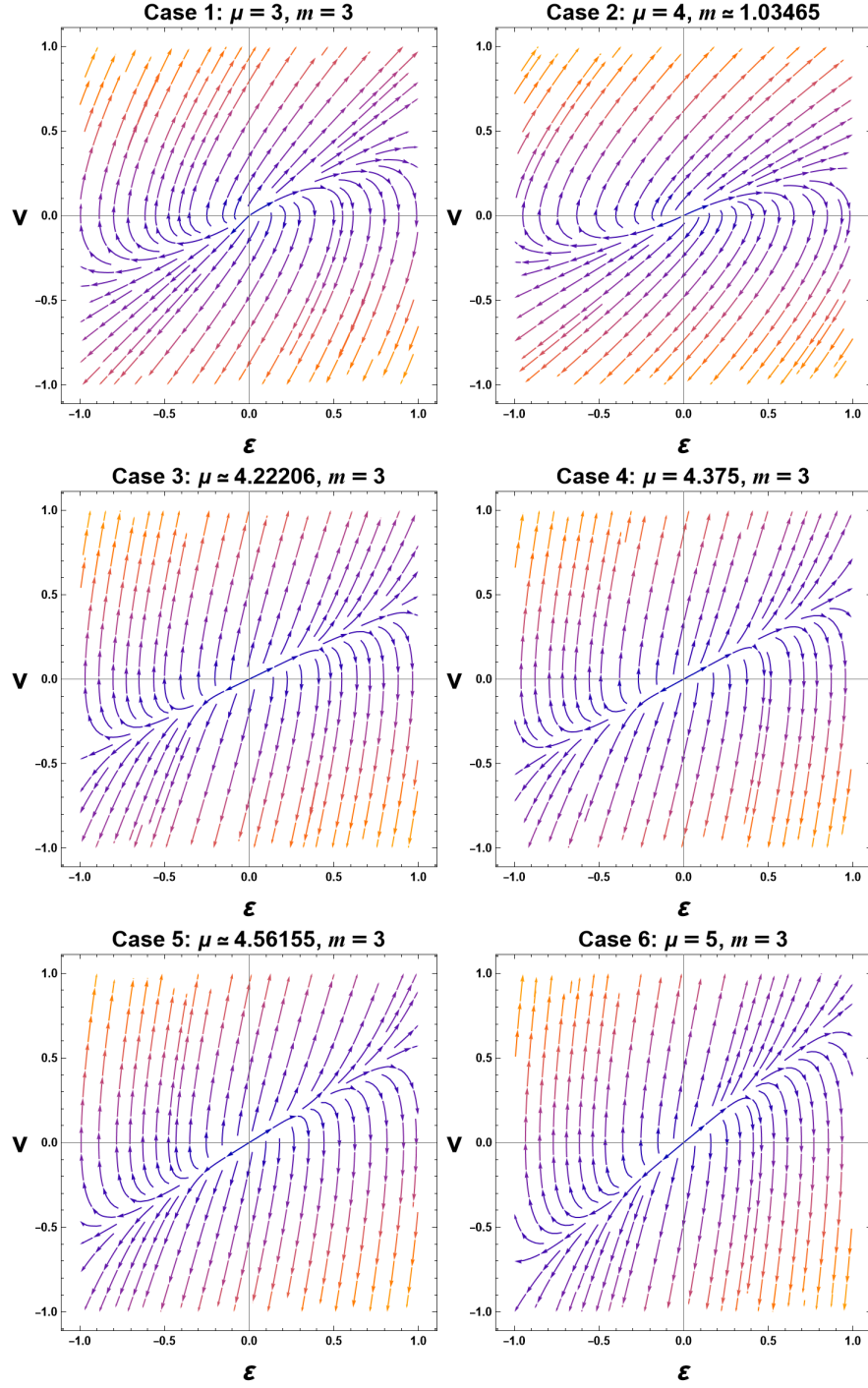


FIG. 4: Flow of system (70)-(71) for the source cases.

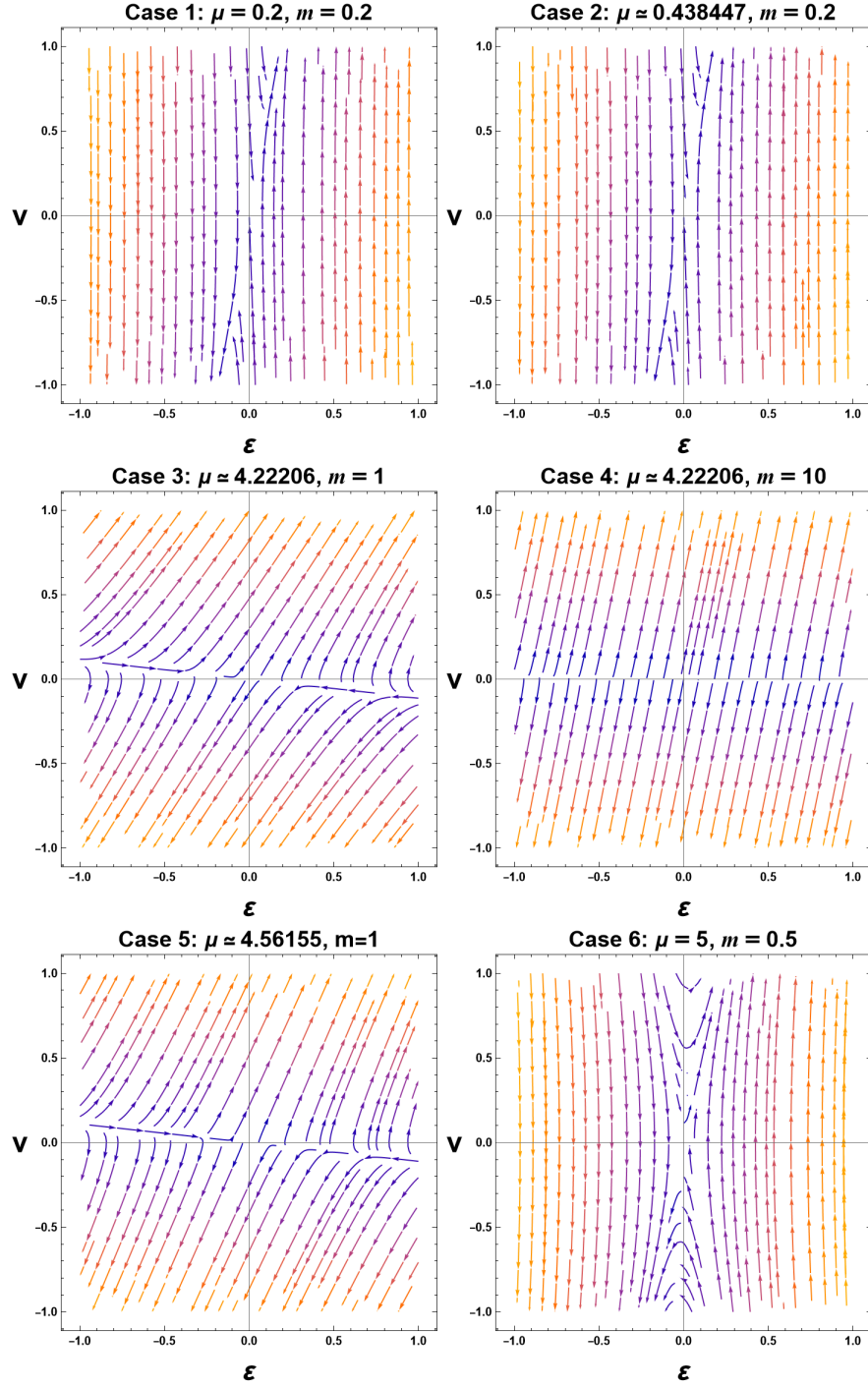


FIG. 5: Flow of system (70)-(71) for the saddle cases.

4.2. Dynamics at infinity

To investigate the late-time dynamics of system (70)-(71) at infinity we define the following variables:

$$X = \frac{\varepsilon}{\sqrt{1 + \varepsilon^2 + v^2}}, Y = \frac{v}{\sqrt{1 + \varepsilon^2 + v^2}}. \quad (74)$$

Hence, we get the system

$$\frac{dX}{d\tau} = \frac{Y}{m^2} \left[m(mX((\mu - 5)\mu X + X + (3 - 2\mu)Y) + m + 2X((15 - 2\mu)X + 2Y)) - 12X^2 \right], \quad (75)$$

$$\begin{aligned} \frac{dY}{d\tau} = & -\frac{1}{m^2} \left[X(m^2((\mu - 5)\mu - ((\mu - 5)\mu + 1)Y^2) + 2) \right. \\ & \left. + 2(2\mu - 15)m(Y^2 - 1) + 12(Y^2 - 1) + mY(Y^2 - 1)((2\mu - 3)m - 4) \right], \end{aligned} \quad (76)$$

defined in the compact set $\{(X, Y) \in \mathbb{R}^2 : X^2 + Y^2 \leq 1\}$.

There are five total equilibrium points for system (75)-(76). However, the existence conditions for each point and their respective eigenvalues depend on both μ and m , therefore the analysis is not trivial. The equilibrium points in the coordinates (X, Y) are

1. $A = (0, 0)$, with eigenvalues (73). The stability analysis is the same as in the finite regime previously performed.
2. $B, C = \left(\pm \frac{k_2 m (k_1 + (2\mu - 3)m - 4)}{\sqrt{k} [2m(-4\mu + ((\mu - 5)\mu + 2)m + 30) - 24]}, \pm \frac{k_2}{\sqrt{k}} \right)$ are antipodal points, where

$$k = 2(\mu^4 - 10\mu^3 + 31\mu^2 - 22\mu + 10)m^4 \quad (77)$$

$$- 8(2\mu^3 - 25\mu^2 + 81\mu - 21)m^3 - 8(2\mu^2 + 30\mu - 223)m^2 + 96(2\mu - 15)m + 288,$$

$$k_1 = \sqrt{m(8\mu m + m - 96) + 64}, \quad (78)$$

$$k_2 = \sqrt{\begin{aligned} & m^3(3(k_1 + 68) - 2\mu(k_1 + 4\mu(2\mu - 25) + 320)) \\ & + 4m^2(k_1 - 4\mu(\mu + 15) + 436) + (2(\mu - 1)\mu((\mu - 9)\mu + 21) + 13)m^4 \\ & + 96(2\mu - 15)m + 288 \end{aligned}}. \quad (79)$$

These points exist for the following intervals

- 1) $\mu = \frac{1}{2}(5 - \sqrt{17})$, $0 \leq m < \frac{1}{83}(60 - 6\sqrt{17})$, or
- 2) $\mu = \frac{1}{2}(5 - \sqrt{17})$, $\frac{1}{83}(60 - 6\sqrt{17}) < m < \frac{8\sqrt{15+4\sqrt{17}-48}}{4\sqrt{17}-21}$, or

- 3) $\mu = \frac{1}{2} (5 - \sqrt{17})$, $m > \frac{-48-8\sqrt{15+4\sqrt{17}}}{4\sqrt{17}-21}$, or
- 4) $\frac{35}{8} < \mu < \frac{1}{2} (5 + \sqrt{17})$, $m > \frac{2\mu-15}{\mu^2-5\mu+2} + \sqrt{\frac{16\mu^2-120\mu+249}{(\mu^2-5\mu+2)^2}}$, or
- 5) $\frac{1}{4} (11 - 2\sqrt{3}) < \mu < \frac{1}{4} (11 + 2\sqrt{3})$, $m > \frac{2\mu-15}{\mu^2-5\mu+2} + \sqrt{\frac{16\mu^2-120\mu+249}{(\mu^2-5\mu+2)^2}}$, or
- 6) $\frac{1}{2} (5 - \sqrt{17}) < \mu < \frac{1}{4} (11 - 2\sqrt{3})$, $m > \frac{2\mu-15}{\mu^2-5\mu+2} + \sqrt{\frac{16\mu^2-120\mu+249}{(\mu^2-5\mu+2)^2}}$, or
- 7) $\mu > \frac{1}{2} (5 + \sqrt{17})$, $m > \frac{2\mu-15}{\mu^2-5\mu+2} + \sqrt{\frac{16\mu^2-120\mu+249}{(\mu^2-5\mu+2)^2}}$, or
- 8) $\frac{1}{4} (11 + 2\sqrt{3}) < \mu \leq \frac{35}{8}$, $m > \frac{2\mu-15}{\mu^2-5\mu+2} + \sqrt{\frac{16\mu^2-120\mu+249}{(\mu^2-5\mu+2)^2}}$, or
- 9) $m = \frac{8(\sqrt{13+4\sqrt{3}}-6)}{4\sqrt{3}-23}$, $\mu = \frac{1}{4} (11 - 2\sqrt{3})$, or
- 10) $\mu = \frac{1}{4} (11 - 2\sqrt{3})$, $0 \leq m < \frac{152+16\sqrt{3}-32\sqrt{13+4\sqrt{3}}}{55+4\sqrt{3}}$, or
- 11) $\mu = \frac{1}{4} (11 - 2\sqrt{3})$, $\frac{152+16\sqrt{3}-32\sqrt{13+4\sqrt{3}}}{55+4\sqrt{3}} < m < \frac{8\sqrt{13+4\sqrt{3}}-48}{4\sqrt{3}-23}$, or
- 12) $\mu = \frac{1}{4} (11 - 2\sqrt{3})$, $m > \frac{-48-8\sqrt{13+4\sqrt{3}}}{4\sqrt{3}-23}$, or
- 13) $m = \frac{8(6+\sqrt{13-4\sqrt{3}})}{23+4\sqrt{3}}$, $\mu = \frac{1}{4} (11 + 2\sqrt{3})$, or
- 14) $\mu = \frac{1}{4} (11 + 2\sqrt{3})$, $0 \leq m < \frac{48-8\sqrt{13-4\sqrt{3}}}{23+4\sqrt{3}}$, or
- 15) $\mu = \frac{1}{4} (11 + 2\sqrt{3})$, $\frac{48+8\sqrt{13-4\sqrt{3}}}{23+4\sqrt{3}} < m < \frac{-152+16\sqrt{3}-32\sqrt{13-4\sqrt{3}}}{4\sqrt{3}-55}$, or
- 16) $\mu = \frac{1}{4} (11 + 2\sqrt{3})$, $m > \frac{-152+16\sqrt{3}-32\sqrt{13-4\sqrt{3}}}{4\sqrt{3}-55}$, or
- 17) $\mu = \frac{1}{2} (5 + \sqrt{17})$, $0 \leq m < -\frac{6}{\sqrt{17}-10}$, or
- 18) $\mu = \frac{1}{2} (5 + \sqrt{17})$, $m > -\frac{6}{\sqrt{17}-10}$, or
- 19) $\mu = \frac{35}{8}$, $m = \frac{4}{3}$, or
- 20) $\mu > \frac{1}{2} (5 + \sqrt{17})$, $0 \leq m < \frac{2\mu-15}{\mu^2-5\mu+2} + \sqrt{\frac{16\mu^2-120\mu+249}{(\mu^2-5\mu+2)^2}}$, or
- 21) $0 \leq \mu < \frac{1}{2} (5 - \sqrt{17})$, $0 \leq m < \frac{2\mu-15}{\mu^2-5\mu+2} + \sqrt{\frac{16\mu^2-120\mu+249}{(\mu^2-5\mu+2)^2}}$, or
- 22) $\frac{1}{4} (11 + 2\sqrt{3}) < \mu \leq \frac{35}{8}$, $0 \leq m < \frac{2\mu-15}{\mu^2-5\mu+2} - \sqrt{\frac{16\mu^2-120\mu+249}{(\mu^2-5\mu+2)^2}}$, or
- 23) $\frac{35}{8} < \mu < \frac{1}{2} (5 + \sqrt{17})$, $0 \leq m < \frac{2\mu-15}{\mu^2-5\mu+2} - \sqrt{\frac{16\mu^2-120\mu+249}{(\mu^2-5\mu+2)^2}}$, or
- 24) $\frac{1}{2} (5 - \sqrt{17}) < \mu < \frac{1}{4} (11 - 2\sqrt{3})$, $0 \leq m < \frac{2\mu-15}{\mu^2-5\mu+2} - \sqrt{\frac{16\mu^2-120\mu+249}{(\mu^2-5\mu+2)^2}}$, or
- 25) $\frac{1}{4} (11 - 2\sqrt{3}) < \mu < \frac{1}{4} (11 + 2\sqrt{3})$, $0 \leq m < \frac{2\mu-15}{\mu^2-5\mu+2} - \sqrt{\frac{16\mu^2-120\mu+249}{(\mu^2-5\mu+2)^2}}$, or
- 26) $0 \leq \mu < \frac{1}{4} (11 - 2\sqrt{3})$, $m = \frac{-64\sqrt{\frac{35-8\mu}{(8\mu+1)^2}}\mu - 8\sqrt{\frac{35-8\mu}{(8\mu+1)^2} + 48}}{8\mu+1}$, or

- 27) $0 \leq \mu < \frac{1}{4} (11 - 2\sqrt{3})$, $m = \frac{-64\sqrt{\frac{35-8\mu}{(8\mu+1)^2}}\mu - 8\sqrt{\frac{35-8\mu}{(8\mu+1)^2} - 48}}{-8\mu-1}$, or
- 28) $0 \leq \mu < \frac{1}{2} (5 - \sqrt{17})$, $\frac{2\mu-15}{\mu^2-5\mu+2} + \sqrt{\frac{16\mu^2-120\mu+249}{(\mu^2-5\mu+2)^2}} < m < \frac{48}{8\mu+1} - 8\sqrt{-\frac{8\mu-35}{(8\mu+1)^2}}$, or
- 29) $0 \leq \mu < \frac{1}{2} (5 - \sqrt{17})$, $m > 8\sqrt{-\frac{8\mu-35}{(8\mu+1)^2}} + \frac{48}{8\mu+1}$, or
- 30) $\frac{1}{4} (11 + 2\sqrt{3}) < \mu < \frac{35}{8}$, $m = \frac{-64\sqrt{\frac{35-8\mu}{(8\mu+1)^2}}\mu - 8\sqrt{\frac{35-8\mu}{(8\mu+1)^2} + 48}}{8\mu+1}$, or
- 31) $\frac{1}{4} (11 + 2\sqrt{3}) < \mu < \frac{35}{8}$, $m = \frac{-64\sqrt{\frac{35-8\mu}{(8\mu+1)^2}}\mu - 8\sqrt{\frac{35-8\mu}{(8\mu+1)^2} - 48}}{-8\mu-1}$, or
- 32) $\frac{1}{4} (11 + 2\sqrt{3}) < \mu \leq \frac{35}{8}$, $\frac{2\mu-15}{\mu^2-5\mu+2} - \sqrt{\frac{16\mu^2-120\mu+249}{(\mu^2-5\mu+2)^2}} < m < \frac{48}{8\mu+1} - 8\sqrt{-\frac{8\mu-35}{(8\mu+1)^2}}$, or
- 33) $\frac{1}{4} (11 + 2\sqrt{3}) < \mu < \frac{35}{8}$, $8\sqrt{-\frac{8\mu-35}{(8\mu+1)^2}} + \frac{48}{8\mu+1} < m < \frac{2\mu-15}{\mu^2-5\mu+2} + \sqrt{\frac{16\mu^2-120\mu+249}{(\mu^2-5\mu+2)^2}}$, or
- 34) $\frac{1}{4} (11 - 2\sqrt{3}) < \mu < \frac{1}{4} (11 + 2\sqrt{3})$, $m = \frac{-64\sqrt{\frac{35-8\mu}{(8\mu+1)^2}}\mu - 8\sqrt{\frac{35-8\mu}{(8\mu+1)^2} + 48}}{8\mu+1}$, or
- 35) $\frac{1}{4} (11 - 2\sqrt{3}) < \mu < \frac{1}{4} (11 + 2\sqrt{3})$, $m = \frac{-64\sqrt{\frac{35-8\mu}{(8\mu+1)^2}}\mu - 8\sqrt{\frac{35-8\mu}{(8\mu+1)^2} - 48}}{-8\mu-1}$, or
- 36) $\frac{1}{4} (11 - 2\sqrt{3}) < \mu < \frac{1}{4} (11 + 2\sqrt{3})$, $\frac{2\mu-15}{\mu^2-5\mu+2} - \sqrt{\frac{16\mu^2-120\mu+249}{(\mu^2-5\mu+2)^2}} < m < \frac{48}{8\mu+1} - 8\sqrt{-\frac{8\mu-35}{(8\mu+1)^2}}$, or
- 37) $\frac{1}{4} (11 - 2\sqrt{3}) < \mu < \frac{1}{4} (11 + 2\sqrt{3})$, $8\sqrt{-\frac{8\mu-35}{(8\mu+1)^2}} + \frac{48}{8\mu+1} < m < \frac{2\mu-15}{\mu^2-5\mu+2} + \sqrt{\frac{16\mu^2-120\mu+249}{(\mu^2-5\mu+2)^2}}$, or
- 38) $\frac{1}{2} (5 - \sqrt{17}) < \mu < \frac{1}{4} (11 - 2\sqrt{3})$, $\frac{2\mu-15}{\mu^2-5\mu+2} - \sqrt{\frac{16\mu^2-120\mu+249}{(\mu^2-5\mu+2)^2}} < m < \frac{48}{8\mu+1} - 8\sqrt{-\frac{8\mu-35}{(8\mu+1)^2}}$, or
- 39) $\frac{1}{2} (5 - \sqrt{17}) < \mu < \frac{1}{4} (11 - 2\sqrt{3})$, $8\sqrt{-\frac{8\mu-35}{(8\mu+1)^2}} + \frac{48}{8\mu+1} < m < \frac{2\mu-15}{\mu^2-5\mu+2} + \sqrt{\frac{16\mu^2-120\mu+249}{(\mu^2-5\mu+2)^2}}$, or
- 40) $\frac{35}{8} < \mu < \frac{1}{2} (5 + \sqrt{17})$, $\frac{2\mu-15}{\mu^2-5\mu+2} - \sqrt{\frac{16\mu^2-120\mu+249}{(\mu^2-5\mu+2)^2}} < m < \frac{2\mu-15}{\mu^2-5\mu+2} + \sqrt{\frac{16\mu^2-120\mu+249}{(\mu^2-5\mu+2)^2}}$.

Recall that the flow in a neighbourhood of antipodal points is topologically equivalent, and it may be reversed [163], but in this case, both points share the same eigenvalues. Therefore, the stability is the same for both B and C . We will write $\lambda_1(B, C) = f_1(\mu, m)$ and $\lambda_2(B, C) = f_2(\mu, m)$, to represent their eigenvalues. Given that many existence conditions and the eigenvalues depend on both free parameters, we will only consider some cases to analyze the stability of B and C . In particular, if we only consider the existence conditions for which the points are hyperbolic (most), we verify by numerical

inspection that the points can never be attractors. However, they can be sources or saddles. When one parameter is fixed and the other free, the behavior is depicted in figure 6. On the other hand, when both parameters are free, the behaviour is shown in figure 7.

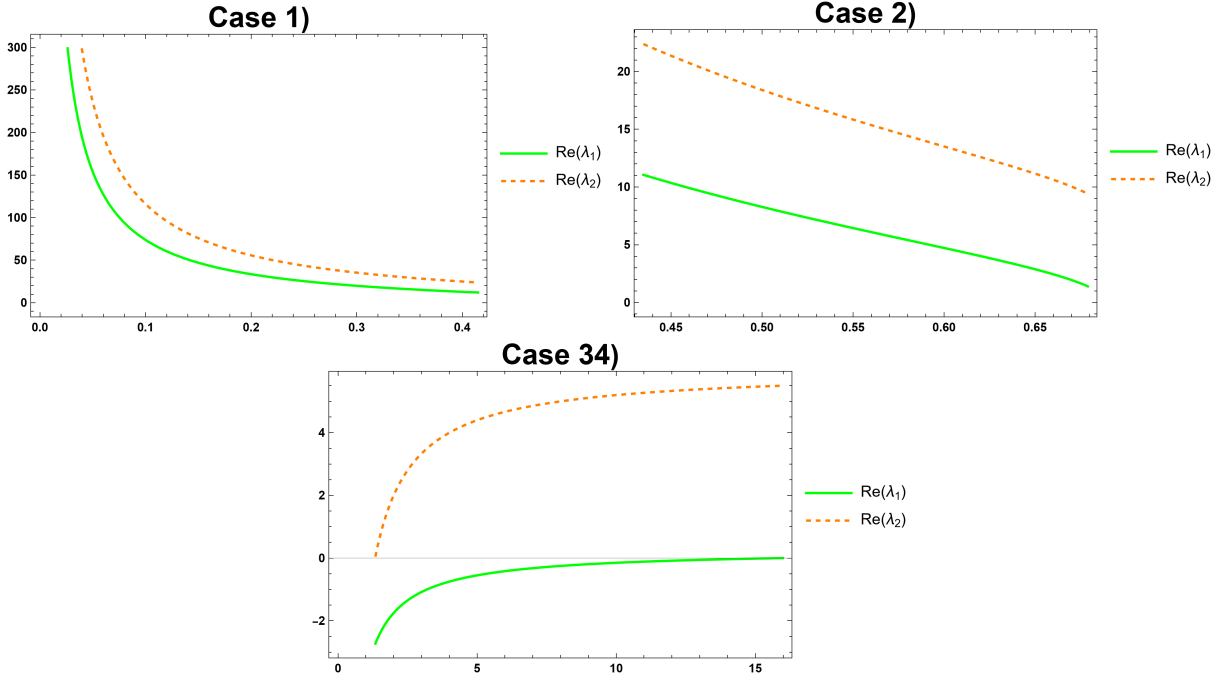


FIG. 6: Real part of the eigenvalues for A and B for a fixed value of one of the parameters according to the respective case. In cases 1) and 2) μ is fixed as $\mu = \frac{1}{2}(5 - \sqrt{17})$ while m moves in two different intervals. In case 34) $\mu = \frac{35}{8}$ and $\frac{4}{5} < m < 16$. Both points behave as sources or saddles whenever they exist and are hyperbolic.

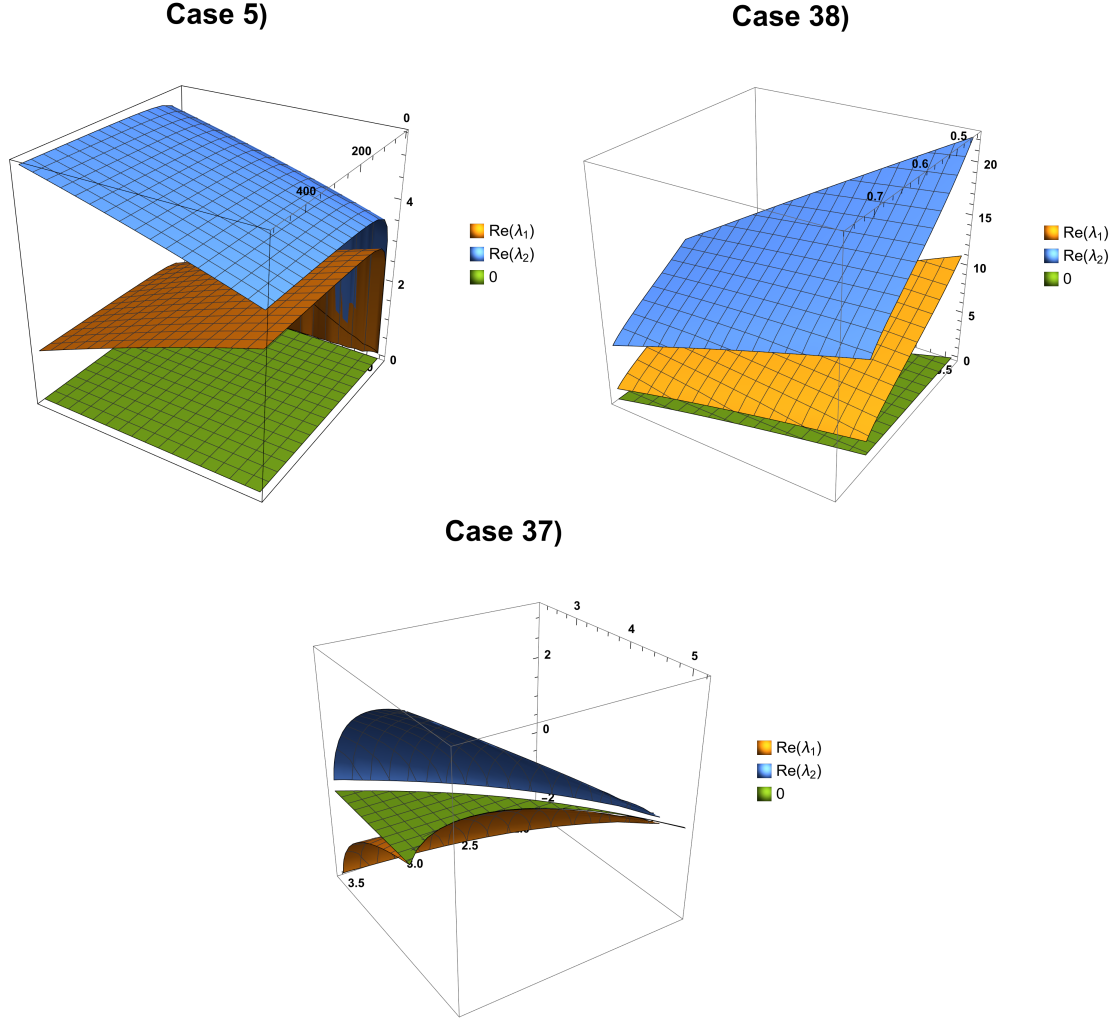


FIG. 7: Real part of the eigenvalues for A and B where both of the parameters μ, m remain free in some intervals. The cases depicted are cases 5), 37) and 38). Once again, as in the figure 6, both points behave either as sources or saddles for every existence condition in which they are hyperbolic.

3. $D, E = \left(\pm \frac{k_2 m [-k_1 + (2\mu - 3)m - 4]}{\sqrt{k} [2m(-4\mu + ((\mu - 5)\mu + 2)m + 30) - 24]}, \frac{k_2}{\sqrt{k}} \right)$, where k and k_1 are defined the same as in (77)-(78) but

$$k_2 = \sqrt{\begin{aligned} & m^3 [k_1(2\mu - 3) - 8\mu(\mu(2\mu - 25) + 80) + 204] \\ & - 4m^2 [k_1 + 4\mu(\mu + 15) - 436] + [2(\mu - 1)\mu((\mu - 9)\mu + 21) + 13] m^4 \\ & + 96(2\mu - 15)m + 288 \end{aligned}}. \quad (80)$$

As before, D and E are antipodal points, and once again, they share the same eigenvalues. We will write them as $\gamma_1 = g_1(\mu, m)$ and $\gamma_2 = g_2(\mu, m)$. The conditions for D and E are the

same as the forty cases. However, D and E can be attractors or saddles in those intervals. Additionally, numerical inspection in every interval shows that the points cannot be sources. See figures 9 and 10.

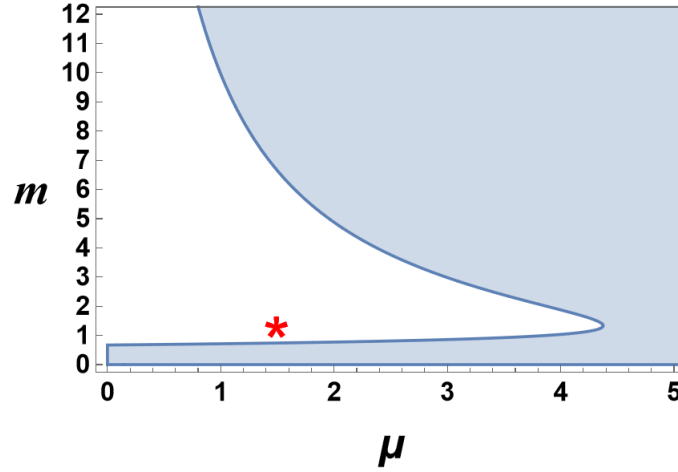


FIG. 8: Existence region for points B , C , D and E . The red star represents the point in the parameter space with the best-fit values of μ and m according to the analysis in §5.

From figure 8 we have that B , C , D , and E do not exist for the best-fit values of μ and m according to the analysis in §5.

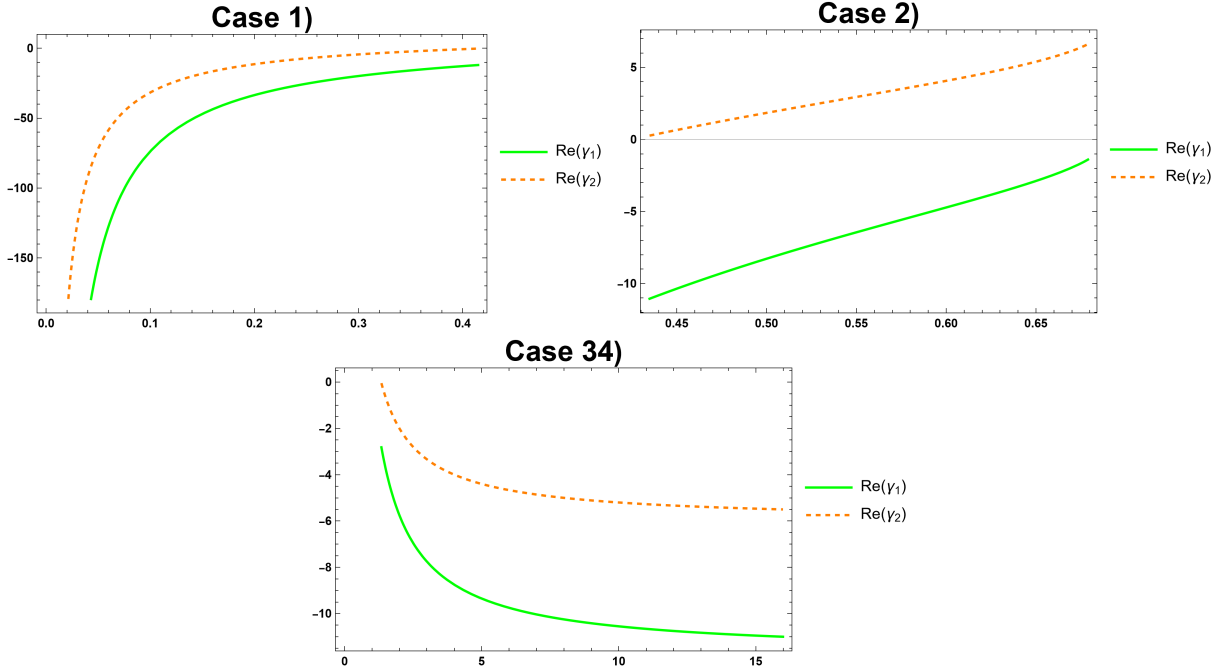


FIG. 9: Real part of the eigenvalues for A and B for a fixed value of one of the parameters according to the respective case. In cases 1) and 2) μ is fixed as $\mu = \frac{1}{2}(5 - \sqrt{17})$ while m moves in two different intervals. In case 34) $\mu = \frac{35}{8}$ and $\frac{4}{5} < m < 16$. Both points behave as sinks or saddles whenever they exist and are hyperbolic.

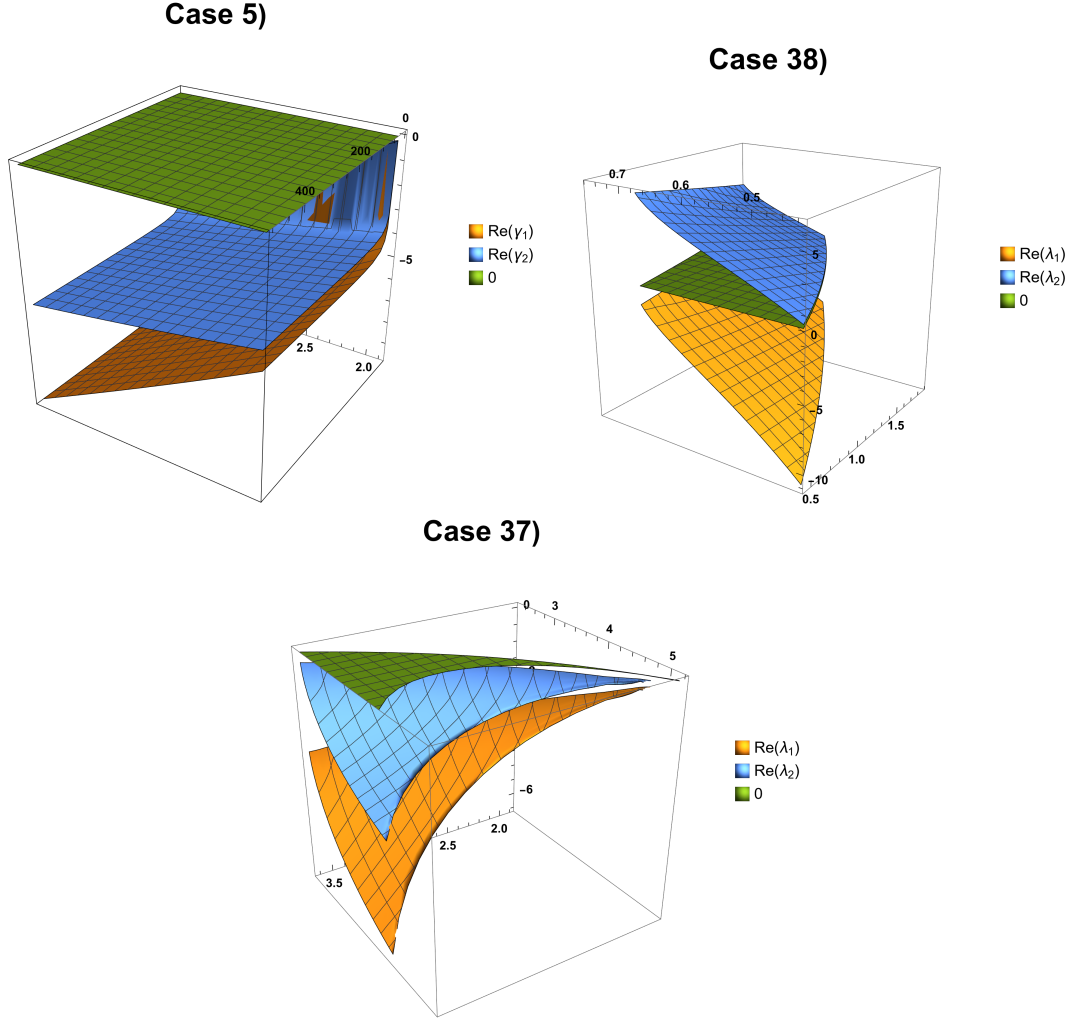


FIG. 10: Real part of the eigenvalues for A and B where both of the parameters μ, m remain free in some intervals. The cases depicted are cases 5), 37) and 38). Once again, as in the figure, 9, both points behave as sinks or saddles whenever they exist and are hyperbolic.

Finally, we get the dynamics shown in figure 11. Here, we observe that the for $\mu = 1, m = 3$ or $\mu = 1, m = 4$ or $\mu = 2, m = 3$ point A is an attractor. However, for $\mu = 2, m = 4$, there are two complex eigenvalues with zero real parts, namely $\left\{ -\frac{i\sqrt{3}}{2}, \frac{i\sqrt{3}}{2} \right\}$ which means A is a center.

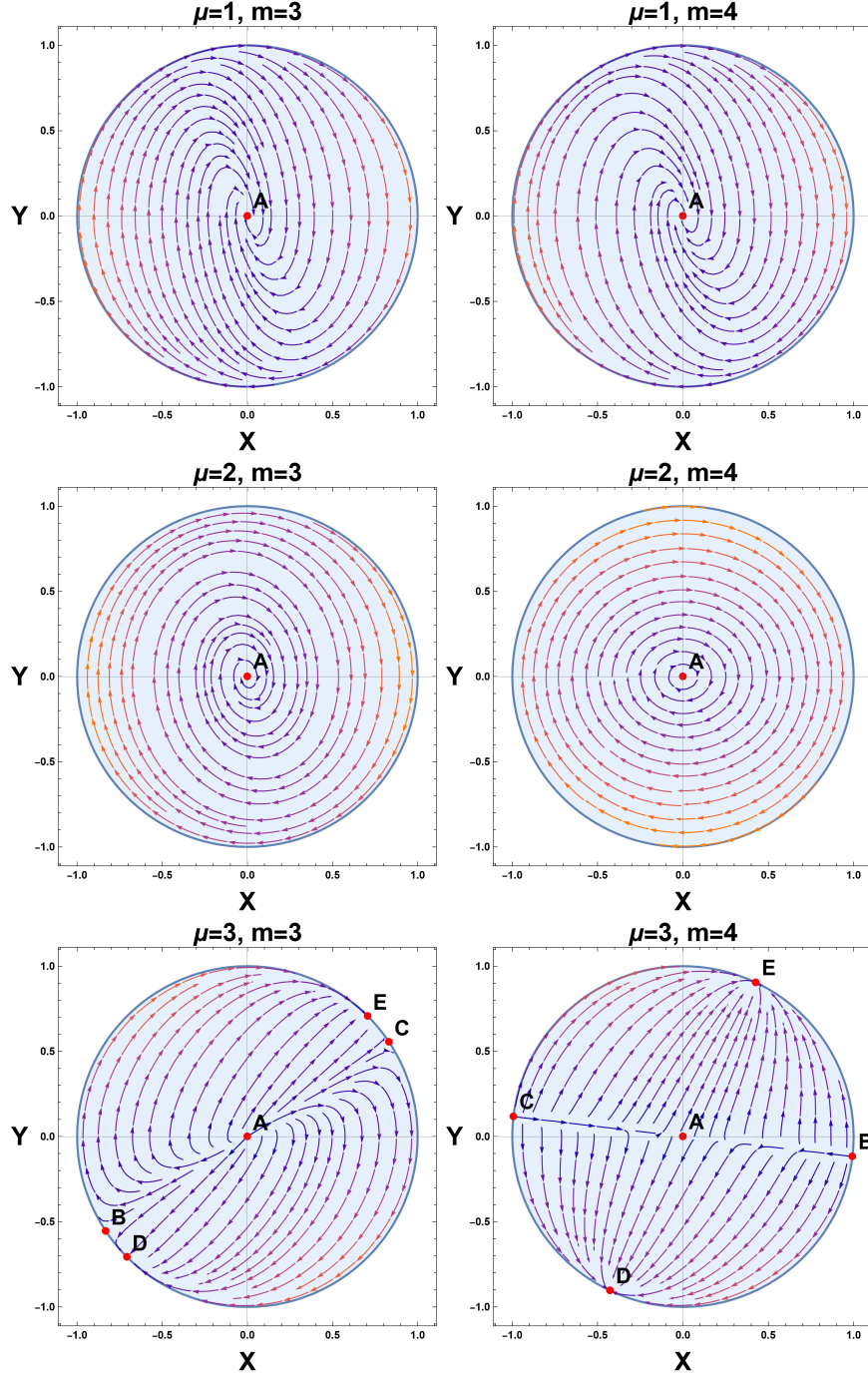


FIG. 11: Dynamics of system (75)-(76) in the compactified region $X^2 + Y^2 \leq 1$ for different values of the parameters μ and m . Some physical values of m were considered, $m = 3$ (dust) $m = 4$ (radiation). We observe that the for $\mu = 1, m = 3$ or $\mu = 1, m = 4$ or $\mu = 2, m = 3$ point A is an attractor. However, for $\mu = 2, m = 4$, there are two complex eigenvalues with zero real parts, namely $\left\{ -\frac{i\sqrt{3}}{2}, \frac{i\sqrt{3}}{2} \right\}$ which means A is a center.

5. OBSERVATIONAL CONSTRAINTS

In this section, we shall constrain the free parameters of the exact scaling solution obtained for the exponential potential (see §3). For that end, we compute the best-fit parameters at 1σ (68.3%) of confidence level (CL) with the affine-invariant Markov chain Monte Carlo (MCMC) method [164], implemented in the pure-Python code *emcee* [165], for the supernovae Ia (SNe Ia), cosmic chronometers (CC), gravitational lensing (GL), and black hole shadows (BHS) data. In this procedure, we have considered 100 chains or “walkers” and the autocorrelation time τ_{corr} , provided by the *emcee* module, as a convergence test. Following this line, we compute at every 50 step the value of τ_{corr} of each free parameter. If the current step is larger than $50\tau_{\text{corr}}$ and the value of τ_{corr} changed by less than 1%, then we will consider that the chains have converged and the constraint is stopped. We discard the first $5\tau_{\text{corr}}$ steps as “burn-in” steps, thin by $\tau_{\text{corr}}/2$, and we flatten the chains. For this MCMC analysis, we consider the following Gaussian likelihood:

$$\mathcal{L}_I \propto \exp\left(-\frac{\chi_I^2}{2}\right), \quad (81)$$

where χ_I^2 is the merit function. In particular, we consider the combinations of data sets χ_{SNe}^2 , $\chi_{\text{SNe+CC}}^2 = \chi_{\text{SNe}}^2 + \chi_{\text{CC}}^2$, and $\chi_{\text{joint}}^2 = \chi_{\text{SNe}}^2 + \chi_{\text{CC}}^2 + \chi_{\text{GL}}^2 + \chi_{\text{BHS}}^2$. As initialization points, we consider a small vicinity around the values that maximized the likelihood.

We first construct the Hubble parameters describing the exact scaling solution in the following subsections. Second, we briefly describe the construction of the merit function of each data set considered in the cosmological constraint. Finally, we present the results and some discussions.

5.1. Hubble parameter for the exponential potential

To obtain the theoretical Hubble parameter for the scaling solution for the exponential potential, we substitute equations (30), (46), and (47) in (24), to obtain

$$\dot{H} = \frac{4(12c_4\lambda^2t^3H^3 + 1)}{3\lambda^2t^2(8c_4t^2H^2 - 1)} - \frac{(\mu - 3)H}{t} - H^2, \quad (82)$$

where,

$$\lambda = \frac{1}{3} \sqrt{\frac{36 - 3m[-4\mu + ((\mu - 5)\mu + 2)m + 30]}{(\mu + 2)m - 6}}, \quad c_4 = \frac{1}{96} m^2 \left[\frac{2m(3\lambda^2 + m)}{\lambda^2[(\mu - 6)m + 2]} + 3 \right].$$

Hence, by introducing the logarithmic independent variable $s = -\ln(1+z)$, for which $s \rightarrow -\infty$ as $z \rightarrow \infty$, $s \rightarrow 0$ as $z \rightarrow 0$, $s \rightarrow \infty$ as $z \rightarrow -1$, and defining the age parameter as $\alpha = tH$, we obtain the initial value problem

$$\alpha'(s) = \frac{2[16c_4\alpha(s) + 3\lambda^2]}{3\lambda^2[8c_4\alpha(s)^2 - 1]} - \mu - \frac{4}{3\lambda^2\alpha(s)} - \alpha(s) + 6, \quad (83)$$

$$t'(s) = t(s)/\alpha(s), \quad (84)$$

$$\alpha(0) := \alpha_0 = t_0H_0, t(0) = t_0. \quad (85)$$

The above system has the exact solution

$$\alpha(s) = \frac{2}{m}, \quad m \neq \frac{6}{\mu}, \quad (86)$$

where $\alpha(0) := \alpha_0 = \frac{2}{m} = t_0H_0$ implies $m = 2/(\alpha_0)$. So, integrating under the initial condition $t(0) = t_0$, we obtain $t(s) = t_0e^{\frac{s}{\alpha_0}}$, and, therefore

$$H(s) = \alpha(s)t(s)^{-1} = H_0e^{-\frac{s}{\alpha_0}} \implies H(z) = H_0(1+z)^{\frac{1}{\alpha_0}}. \quad (87)$$

Finally, from equation (25), we have the effective matter sources:

$$\Omega_\phi := \frac{\frac{1}{2}\dot{\phi}^2 + V(\phi)}{3H^2} = 1 - \frac{2\alpha_0(3\alpha_0 - \mu - 6) + 4(\mu - 1)}{\alpha_0[2\alpha_0\mu + 3\alpha_0(\alpha_0 - 5) - \mu^2 + 5\mu - 2]}, \quad (88)$$

and

$$\begin{aligned} \Omega_X &:= \Omega_{\text{fracc}} + \Omega_{\text{GB}} + \Omega_{\text{GB,fracc}} = \frac{-\frac{3(\mu-1)H(8H^2\psi-1)}{t} + 24H^3\dot{\psi}}{3H^2} \\ &= \frac{2\alpha_0(3\alpha_0 - \mu - 6) + 4(\mu - 1)}{\alpha_0[2\mu\alpha_0 + 3\alpha_0(\alpha_0 - 5) - \mu^2 + 5\mu - 2]}, \end{aligned} \quad (89)$$

with

$$\Omega_\phi + \Omega_X = 1, \quad (90)$$

where, for this scaling solution, the scalar field behaves as dark matter, say

$$\Omega_\phi = \Omega_{DM}, \quad (91)$$

and the extra terms $\Omega_{\text{fracc}} + \Omega_{\text{GB}} + \Omega_{\text{GB,fracc}}$ mimics dark energy Ω_X .

To compare with the fractional cosmological model, we also constraint the Λ CDM model whose respective theoretical Hubble parameter is given by

$$H = H_0\sqrt{\Omega_{m,0}(1+z)^3 + 1 - \Omega_{m,0}}, \quad (92)$$

whose respective parameter space is $\boldsymbol{\theta} = (H_0, \Omega_{m,0})$.

For this scaling solution (86), we have that Ω_ϕ and Ω_X are constants. Therefore,

$$1 - \frac{2\alpha_0(3\alpha_0 - \mu - 6) + 4(\mu - 1)}{\alpha_0[2\alpha_0\mu + 3\alpha_0(\alpha_0 - 5) - \mu^2 + 5\mu - 2]} = \Omega_{m,0}. \quad (93)$$

Hence, we have two solutions

$$\begin{aligned} \mu_{\pm} = & \frac{1}{2\alpha_0(\Omega_{m,0} - 1)} \left\{ \alpha_0(2\alpha_0(\Omega_{m,0} - 1) + 5\Omega_{m,0} - 7) + 4 \right. \\ & \left. \pm \sqrt{\alpha_0 \left[\alpha_0 \left(16\alpha_0^2(\Omega_{m,0} - 1)^2 - 8\alpha_0(5\Omega_{m,0} - 7)(\Omega_{m,0} - 1) \right) \right. \right.} \\ & \left. \left. + \Omega_{m,0}(17\Omega_{m,0} - 86) + 73 \right] + 8(3\Omega_{m,0} - 5) \right\} + 16 \quad (94) \end{aligned}$$

Therefore, we use a Bayesian analysis to obtain the best-fit values of $\Omega_{m,0}$ and α_0 , and substitute in the previous expressions to obtain the physical values of μ .

5.2. Cosmic Chronometers

To constrain the model with CC, we consider the data set of Ref. [166], which consists of 31 data points in the redshift range $0.0708 \leq z \leq 1.965$. These Hubble data points are obtained by the differential age method, which is a model-independent method [167]. Hence, the merit function for the CC data is constructed as

$$\chi_{CC}^2 = \sum_{i=1}^{31} \left[\frac{H_i - H_{th}(z_i, \boldsymbol{\theta})}{\sigma_{H,i}} \right]^2, \quad (95)$$

where H_i is the observational Hubble parameter at redshift z_i with an associated error $\sigma_{H,i}$, all of them provided by the CC sample, H_{th} is the theoretical Hubble parameter at the same redshift, and $\boldsymbol{\theta}$ encompasses the free parameters of the model.

Note that the same theoretical Hubble parameter gives both analytical solutions of interest for the cosmological constraint, according to the Eq. (87) whose parameter space is $\boldsymbol{\theta} = (H_0, \alpha_0)$. Therefore, we consider for our MCMC analysis the flat priors $0.55 < h < 0.85$ and $0.5 < \alpha_0 < 2.5$, where h is the reduced Hubble constant according to the expression $H_0 = 100 \frac{km/s}{Mpc} h$. We also constraint the Λ CDM model as a further comparison, whose respective theoretical Hubble parameter is given by (92), whose respective parameter space is $\boldsymbol{\theta} = (H_0, \Omega_{m,0})$, for which we consider the same prior on h as in the fractional cosmology, plus the flat prior $0 < \Omega_{m,0} < 1$.

5.3. Type Ia supernovae

For the SNe Ia data, we consider the Pantheon+ sample [168], which consists of 1701 data points in the redshift range $0.001 \leq z \leq 2.26$, whose respective merit function can be conveniently constructed in matrix notation (denoted by bold symbols) as

$$\chi_{\text{SNe}}^2 = \mathbf{\Delta D}(z, \boldsymbol{\theta}, M)^\dagger \mathbf{C}^{-1} \mathbf{\Delta D}(z, \boldsymbol{\theta}, M), \quad (96)$$

where $[\mathbf{\Delta D}(z, \boldsymbol{\theta}, M)]_i = m_{B,i} - M - \mu_{th}(z_i, \boldsymbol{\theta})$ and $\mathbf{C} = \mathbf{C}_{\text{stat}} + \mathbf{C}_{\text{sys}}$, with \mathbf{C} the total uncertainty covariance matrix. The matrices \mathbf{C}_{stat} and \mathbf{C}_{sys} account for the statistical and systematic uncertainties, respectively. The quantity $\mu_i = m_{B,i} - M$ corresponds to the observational distance modulus of the Pantheon+ sample, which is obtained by a modified version of Trip’s formula [169] and the BBC (BEAMS with Bias Corrections) approach [170]. In contrast, $m_{B,i}$ is the corrected apparent B-band magnitude of a fiducial SNe Ia at redshift z_i , and M is the fiducial magnitude of an SNe Ia, which must be jointly estimated with the free parameters of the model under study.

The theoretical distance modulus for a spatially flat FLRW spacetime is given by

$$\mu_{th}(z_i, \boldsymbol{\theta}) = 5 \log_{10} \left[\frac{d_L(z_i, \boldsymbol{\theta})}{\text{Mpc}} \right] + 25, \quad (97)$$

with $d_L(z_i, \boldsymbol{\theta})$ the luminosity distance given by

$$d_L(z_i, \boldsymbol{\theta}) = c(1 + z_i) \int_0^{z_i} \frac{dz'}{H_{th}(z', \boldsymbol{\theta})}, \quad (98)$$

where c is the speed of light given in units of km/s.

In principle, there is a degeneration between M and H_0 . Hence, to constraint H_0 using SNe Ia data alone, it is necessary to include the SH0ES (Supernovae and H_0 for the Equation of State of the dark energy program) Cepheid host distance anchors, with a merit function of the form

$$\chi_{\text{Cepheid}}^2 = \mathbf{\Delta D}_{\text{Cepheid}}(M)^\dagger \mathbf{C}^{-1} \mathbf{\Delta D}_{\text{Cepheid}}(M), \quad (99)$$

where $[\mathbf{\Delta D}_{\text{Cepheid}}(M)]_i = \mu_i(M) - \mu_i^{\text{Cepheid}}$, with μ_i^{Cepheid} the Cepheid calibrated host-galaxy distance obtained by SH0ES [171]. So, we use the Cepheid distances as the “theory model” to calibrate M , considering that the difference $\mu_i(M) - \mu_i^{\text{Cepheid}}$ is sensitive to M and largely insensitive to other parameters of the cosmological model. Considering the total uncertainty

covariance matrix for Cepheid is contained in the total uncertainty covariance matrix \mathbf{C} , we can define the merit function for the SNe Ia data as

$$\chi_{\text{SNe}}^2 = \mathbf{\Delta D}'(z, \boldsymbol{\theta}, M)^\dagger \mathbf{C}^{-1} \mathbf{\Delta D}'(z, \boldsymbol{\theta}, M), \quad (100)$$

where

$$\Delta \mathbf{D}'_i = \begin{cases} m_{B,i} - M - \mu_i^{\text{Cepheid}} & i \in \text{Cepheid host} \\ m_{B,i} - M - \mu_{th}(z_i, \boldsymbol{\theta}) & \text{otherwise} \end{cases}. \quad (101)$$

For the nuisance parameter M , we consider the flat prior $-20 < M < -18$ in our MCMC analysis.

5.4. Gravitational lensing

When a background object (the source) is lensed due to the gravitational force of an intervening massive body (the lens), it is obtained the generation of multiple images. Therefore, the light rays emitted from the source will take different paths through space-time at different image positions and arrive at the observer at different times. In this sense, the time delay of two different images k and l depends on the mass distribution along the line of sight of the lensing object and can be calculated as

$$\Delta t_{kl} = \frac{D_{\Delta t}}{c} \left[\frac{(\phi_k - \beta)^2}{2} - \psi(\phi_k) - \frac{(\phi_l - \beta)^2}{2} + \psi(\phi_l) \right], \quad (102)$$

where ϕ_k and ϕ_l are the angular position of the images, β is the angular position of the source, $\psi(\phi_k)$ and $\psi(\phi_l)$ are the lens potential at the image positions, and $D_{\Delta t}$ is the ‘‘time-delay distance’’, which is theoretically given by the expression [172]

$$D_{\Delta t}^{th}(\mathbf{z}, \boldsymbol{\theta}) = (1 + z_l) \frac{d_{A,l}(z_l, \boldsymbol{\theta}) d_{A,s}(z_s, \boldsymbol{\theta})}{d_{A,ls}(z_{ls}, \boldsymbol{\theta})}, \quad (103)$$

where the subscripts l , s , and ls stand for the lens, the source, and between the lens and the source, respectively, $\mathbf{z} = (z_l, z_s, z_{ls})$, and $d_{A,j}$ is the angular diameter distance, which can be written in terms of the luminosity distance (98) as $d_L(z_j, \boldsymbol{\theta}) = d_{A,j}(1 + z_j)^2$ or

$$d_{A,j}(z_j, \boldsymbol{\theta}) = \frac{c}{(1 + z_j)} \int_0^{z_j} \frac{dz'}{H_{th}(z', \boldsymbol{\theta})}. \quad (104)$$

In this paper, we consider the gravitational lensing compilation provided by the H0LiCOW collaboration [173], which consists of six lensed quasars: B1608+656 [174], SDSS 1206+4332

[175], WFI2033-4723 [176], RXJ1131-1231, HE 0435-1223, and PG 1115-080 [177]; whose respective merit function can be constructed as

$$\chi_{\text{GL}}^2 = \sum_{i=1}^6 \left[\frac{D_{\Delta t,i} - D_{\Delta t}^{\text{th}}(\mathbf{z}_i, \boldsymbol{\theta})}{\sigma_{D_{\Delta t,i}}} \right]^2, \quad (105)$$

where $D_{\Delta t,i}$ is the observational time-delay distance of the lensed quasar at redshift $\mathbf{z}_i = (z_{l,i}; z_{s,i}; z_{ls,i})$ with an associated error $\sigma_{D_{\Delta t,i}}$ (for more details see Ref. [173]). It is important to note that, for $z \rightarrow 0$, the angular diameter distance (104) tends to $d_A \rightarrow cz/H_0$ and, therefore, the gravitational lensing data of the H0LiCOW collaboration is sensitive to H_0 , with a weak dependency on other cosmological parameters.

5.5. Black hole shadows

The BHS data is of interest to study our local universe since their dynamic is quite simple and can be seen as standard rulers if the angular size redshift α , the relation between the size of the shadow and the mass of the supermassive black hole that produces it, is established [178]. In this paper, we are interested in two measures: the first one was made on the M87* supermassive black hole by The Event Horizon Telescope Collaboration [179] (the first detection of a BHS) and the second one correspond to the detection of Sagittarius A* (Sgr A*) [180].

Light rays curve around its event horizon in a black hole (BH), creating a ring with a black spot center, the so-called shadow of the BH. The angular radius of the BHS for a Schwarzschild (SH) BH at redshift z_i is given by

$$\alpha_{SH}(z_i, \boldsymbol{\theta}) = \frac{3\sqrt{3}m}{d_A(z_i, \boldsymbol{\theta})}, \quad (106)$$

where $d_A(z_i, \boldsymbol{\theta})$ is given by Eq. (104) (note that the sub-index j is not necessary in this case) and $m = GM_{BH}/c^2$ is the mass parameter of the BH, with M_{BH} the mass of the BH in solar masses units and G the gravitational constant.

It is common to write Eq. (106) in terms of the shadow radius $\alpha_{SH}(z_i, \boldsymbol{\theta}) = R_{SH}/d_A(z_i, \boldsymbol{\theta})$, where $R_{SH} = 3\sqrt{3}GM_{BH}/c^2$ (the speed of light is given in units of m/s in this case). Therefore, the merit function for the BHS data can be constructed as

$$\chi_{BHS}^2 = \sum_{i=1}^2 \left[\frac{\alpha_i - \alpha_{SH}(z_i, \boldsymbol{\theta})}{\sigma_{\alpha,i}} \right]^2, \quad (107)$$

where α_i is the observational angular radius of the BHS at redshift z_i with an associated error $\sigma_{\alpha,i}$. It is important to note that for $z \rightarrow 0$ the angular radius (106) tends to $\alpha_{SH} \rightarrow R_{SH}H_0/cz$ and, therefore, as well as in the gravitational lensing data, the BHS data is sensitive to H_0 , with a weak dependency on other cosmological parameters. On the other hand, we divide Eq. (106) by a factor of 1.496×10^{11} to obtain α_{SH} in units of μas .

5.6. Results and discussion

In Table I, we present the total number of steps and the correlation time for the free parameters space of the Λ CDM and the fractional cosmology. In Table II, we present their respective best-fit values at 1σ CL and χ^2_{\min} criteria. In Figs. 12 and 13, we depict the posterior 1D distribution and joint marginalized regions of the free parameters space of the Λ CDM and fractional cosmologies at 1σ , 2σ (95.5%), and 3σ (99.7%) CL, respectively. These results were obtained by the MCMC analysis described in §5 for the SNe Ia, SNe Ia+CC, and SNe Ia+CC+GL+BHS (joint) data.

Data	Total steps	τ_{corr}			
		h	$\Omega_{m,0}$	α_0	M
Λ CDM cosmology					
SNe Ia	1250	24.3	22.7	...	24.3
SNe Ia+CC	1300	25.2	24.3	...	25.0
joint	1350	23.4	24.6	...	23.6
Fractional cosmology					
SNe Ia	1300	24.5	...	25.0	24.6
SNe Ia+CC	1600	25.0	...	26.3	25.5
joint	1350	24.8	...	23.0	24.3

TABLE I: Total number of steps and autocorrelation time τ_{corr} for the free parameters space of the Λ CDM and the fractional cosmology, respectively. These values were obtained when the convergence test described in §5 is fulfilled for an MCMC analysis with 100 chains and the flat priors $0.55 < h < 0.85$, $0 < \Omega_{m,0} < 1$, $0.5 < \alpha_0 < 2.5$, and $-20 < M < -18$. This information is provided so that our results are replicable.

Data	Best-fit values				χ_{\min}^2
	h	$\Omega_{m,0}$	α_0	M	
Λ CDM cosmology					
SNe Ia	0.734 ± 0.010	0.333 ± 0.018	\dots	-19.25 ± 0.03	1523
SNe Ia+CC	0.719 ± 0.009	0.314 ± 0.016	\dots	-19.30 ± 0.03	1547
Joint	0.724 ± 0.008	0.311 ± 0.016	\dots	-19.28 ± 0.02	1681
Fractional cosmology					
SNe Ia	0.729 ± 0.010	\dots	1.41 ± 0.06	-19.25 ± 0.03	1532
SNe Ia+CC	0.717 ± 0.009	\dots	1.39 ± 0.05	-19.28 ± 0.02	1564
Joint	0.712 ± 0.007	\dots	1.38 ± 0.05	-19.29 ± 0.02	1706

TABLE II: Best-fit values and χ_{\min}^2 criteria of the Λ CDM and the fractional cosmology respectively, for the SNe Ia, SNe Ia+CC, and SNe Ia+CC+GL+BHS (joint) data. The uncertainties presented correspond to 1σ CL.

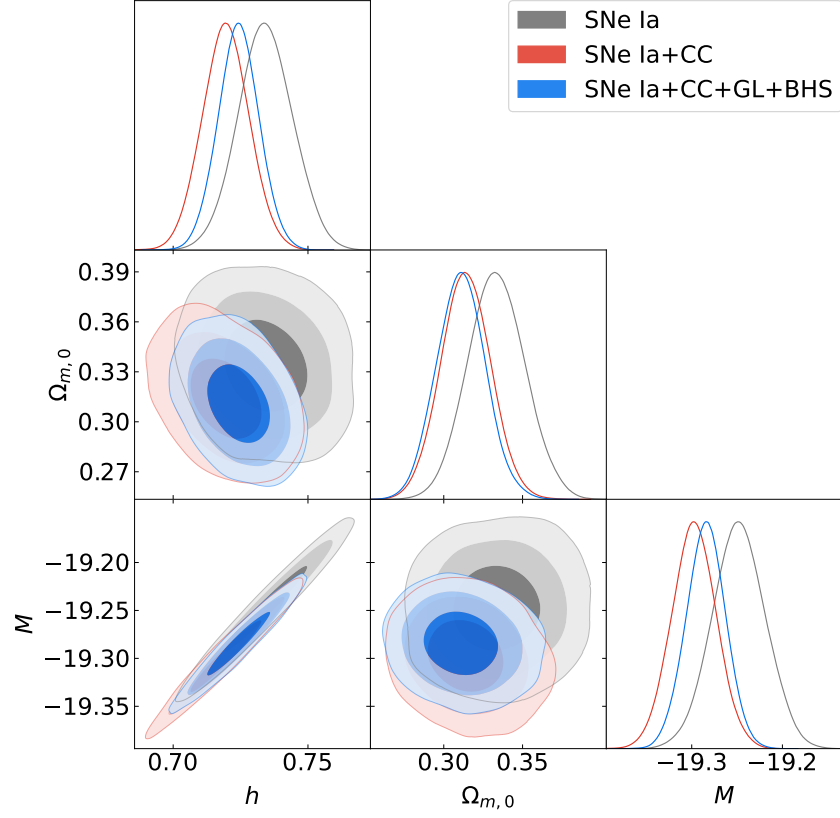


FIG. 12: Posterior 1D distribution and joint marginalized regions of the free parameters space of the Λ CDM cosmology for the SNe Ia, SNe Ia+CC, and SNe Ia+CC+GL+BHS (joint) data. The admissible joint regions correspond to 1 σ , 2 σ , and 3 σ CL, respectively. The best-fit values for each model free parameter are shown in Table II.

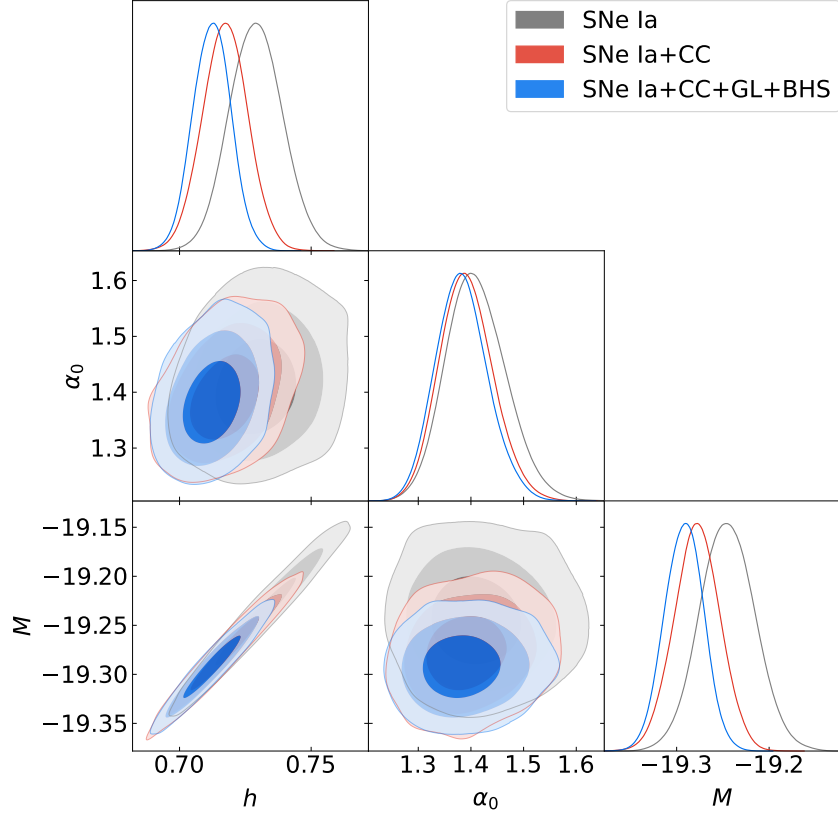


FIG. 13: Posterior 1D distribution and joint marginalized regions of the free parameters space of the fractional cosmology for the SNe Ia, SNe Ia+CC, and SNe Ia+CC+GL+BHS (joint) data. The admissible joint regions correspond to 1σ , 2σ , and 3σ CL, respectively. The best-fit values for each model free parameter are shown in Table II.

In Table II, we can see that the Λ CDM model exhibits lower values of the χ_{\min}^2 criteria compared to the scaling solution explored in this paper. However, it is essential to note that this solution does not fully represent the behavior of the fractional cosmology studied in this paper. It only provides an approximate solution to the complete picture. Therefore, the constraint presented in the table offers insights into the ability of this fractional cosmology to describe the observed Universe. An explanation of this behavior can be seen in Figure 14, where we depict the Hubble parameter for the Λ CDM cosmology and the fractional cosmology for the exponential potential as a function of the redshift z . The figure shows that the solution can only mimic the Λ CDM model at a redshift $z < 0.5$. From this point, the solutions are moving away, with the differences being greater when the redshift increases.

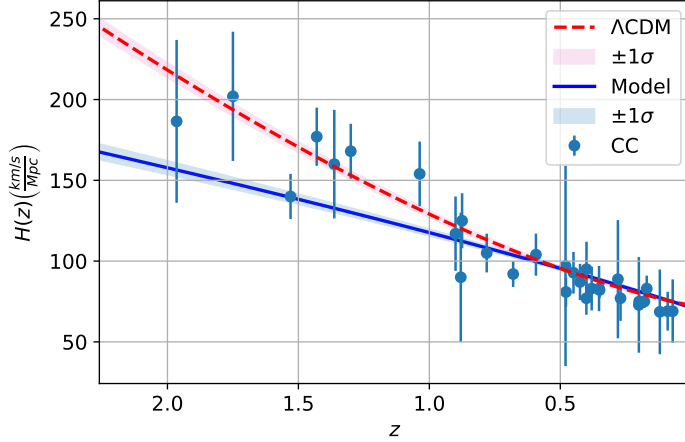


FIG. 14: Theoretical Hubble parameter for the Λ CDM cosmology (red dashed line) and the fractional cosmology for the exponential potential (solid blue line) as a function of the redshift z , contrasted with the CC sample. The shaded curve represents the confidence regions of the Hubble parameter at a 1σ CL. The figure was obtained using the chains of the MCMC procedure described in §5 for the joint analysis.

To reconstruct the other parameters that characterized the solution, we use the chains obtained in our MCMC analysis described in §5 for the fractional cosmology in the case of the joint analysis. Following this line, considering that $\alpha = 2/m$, we obtain at 1σ CL the value $m = 1.44 \pm 0.05$. Also, considering that $\alpha_0 = t_0 H_0$, we obtain at 1σ CL the value $t_0 = 19.0 \pm 0.7$ [Gyr]. On the other hand, to infer the value of μ for the scaling solution obtained for the exponential potential, we also consider the chains obtained in our MCMC analysis described in §5 for the Λ CDM model in the case of the joint analyzing. Therefore, from Eq. (88), we obtain the approximated values $\mu = 1.491$ and $\mu = 4.974$.

Focusing on the observational suitable solution for the joint analysis, in Figure 15, we depict the deceleration parameter for the fractional cosmology obtained for the exponential potential as a function of the redshift z , with an error band at 1σ CL. We also depict the deceleration parameter for the Λ CDM cosmology as a reference model. From this figure, we can conclude that this solution only represents an always expanding solution and does not exhibit a transition between a decelerated solution and an accelerated one as the Λ CDM model. The deceleration parameter for this fractional solution is constant and given by $q = -1 + \alpha_0^{-1}$, with a value at 1σ CL of $q_0 = -0.28 \pm 0.03$ at the current time, i.e., this

solution also represents a less accelerated solution than the Λ CDM cosmology at the current time. Nevertheless, we must again emphasize that this solution is only a particular solution and does not represent the complete picture of fractional cosmology. This solution sheds some light on the capability of fractional cosmology in describing the cosmological background where, as we can see, we can obtain an accelerated solution at the current time without invoking some dark energy.

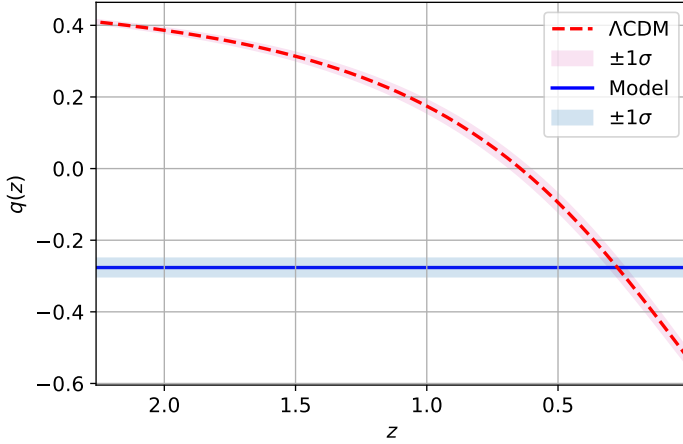


FIG. 15: Deceleration parameters for the Λ CDM cosmology (red dashed line) and the fractional cosmology for the exponential potential (solid blue line) as a function of the redshift z . The shaded curves represent the confidence region of the deceleration parameter at a 1σ CL. The figure was obtained using the chains of the MCMC procedure described in §5 for the joint analysis.

Finally, we construct the $\mathbb{H}0(z)$ diagnostic [181] for the observational suitable fractional solution, which can give us insights about the possibility of alleviating the H_0 tension. Following this line, the $\mathbb{H}0(z)$ diagnostic is defined by

$$\mathbb{H}0(z) = H(z)/\sqrt{\Omega_{m,0}(1+z)^3 + 1 - \Omega_{m,0}}, \quad (108)$$

where the Hubble parameter is obtained numerically by $H(z) = H_{th}(z)$ as we explained before. So, in Figure 16, we depict the $\mathbb{H}0$ diagnostic for the Λ CDM cosmology and the fractional solution as a function of the redshift z , with an error band at 1σ CL. This figure shows that at redshift $z > 0.5$ (the same redshift where both models are moving away according to Figure 14), the value of $H0$ for the fractional cosmology presents a running to values lower

than $H_0 = 74.03 \pm 1.42 \frac{\text{km/s}}{\text{Mpc}}$, obtained by model-independent measurements of cepheid [182]. Therefore, fractional cosmology can be a suitable framework to alleviate the H_0 tension.

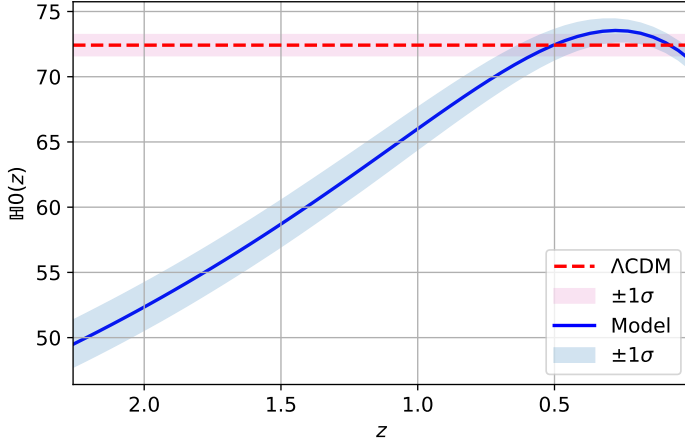


FIG. 16: H_0 diagnostics for the Λ CDM cosmology (red dashed line) and the fractional cosmology for the exponential potential (solid blue line) as a function of the redshift z . The shaded curve represents the confidence regions of the H_0 diagnostic at a 1σ CL. The figure was obtained using the chains of the MCMC procedure described in §5 for the joint analysis.

6. CONCLUDING REMARKS

In this paper, we introduced a new theory called fractional Einstein-Gauss-Bonnet scalar field gravity, which has significant implications for cosmology. We derived a modified Friedmann and Klein-Gordon equations using fractional calculus to change the gravitational action integral in §2. Our research reveals non-trivial solutions associated with exponential potential, exponential couplings to the Gauss-Bonnet term, and logarithmic scalar field. Ultimately, we obtained late-time accelerating power-law solutions for the scale factor and Hubble parameter with inverse time power-law expansion in §3. We reveal the structure of the phase space by employing linear stability theory and analyze the dynamical effects of the Gauss-Bonnet couplings. The stability analysis of the solutions is a crucial aspect of our research, which was performed in §4, where we presented a reconstruction procedure for the potential and the coupling functions. To reconstruct the other parameters that characterized the solution, we used the chains obtained in our MCMC analysis described in §5 for the fractional cosmology in the case of the joint analysis. Following this line, considering that

$\alpha = 2/m$, we obtained at 1σ CL the value $m = 1.44 \pm 0.05$. Also, considering that $\alpha_0 = t_0 H_0$ in both solutions, we obtained at 1σ CL the value $t_0 = 19.0 \pm 0.7$ [Gyr]. On the other hand, to infer the value of μ for the scaling solution obtained for the exponential potential, we also considered the chains obtained in our MCMC analysis described in §5 for the Λ CDM model in the case of the joint analyzing. Therefore, from Eq. (88), we obtained the approximated values $\mu = 1.491$ and $\mu = 4.974$.

Focusing on the observational suitable solution for the joint analysis, we depicted the deceleration parameter for the fractional cosmology obtained for the exponential potential as a function of the redshift z , with an error band at 1σ CL. We used the Λ CDM cosmology as a reference model. We concluded that this solution represents a constantly expanding solution and does not exhibit a transition from a decelerated solution to an accelerated one as the Λ CDM model. The deceleration parameter for this fractional solution is constant and given by $q = -1 + \alpha_0^{-1}$, with a value at 1σ CL of $q_0 = -0.28 \pm 0.03$ at the current time, i.e., this solution also represents a less accelerated solution than the Λ CDM cosmology at the current time. Nevertheless, we must again emphasize that this solution is only a particular solution and does not represent the complete picture of fractional cosmology. This solution sheds some light on the capability of fractional cosmology in describing the cosmological background where, as we can see, we can obtain an accelerated solution at the current time without invoking some dark energy.

Finally, we construct the $\mathbb{H}0(z)$ diagnostic [181] for the observational suitable fractional solution, which gave us insights about the possibility of alleviating the H_0 tension. Following this line, the $\mathbb{H}0(z)$ diagnostic (108), where the Hubble parameter is obtained numerically by $H(z) = H_{th}(z)$. We depicted the $\mathbb{H}0$ diagnostic for the Λ CDM cosmology and the fractional solution as a function of the redshift z , with an error band at 1σ CL. We have shown that at redshift $z > 0.5$, the value of $H0$ for the fractional cosmology presents a running to values lower than $H_0 = 74.03 \pm 1.42 \frac{km/s}{Mpc}$, obtained by model-independent measurements of cepheid [182]. Therefore, fractional cosmology can be a suitable framework to alleviate the H_0 tension.

Summarizing, our model presents several classes of equilibrium points corresponding to different cosmological scenarios, such as accelerated and scaling solutions. The scaling behavior at some equilibrium points revealed that the geometric corrections in the coupling to the Gauss-Bonnet scalar can mimic the behavior of the dark sector in modified gravity.

Our results generalize and significantly improve previous achievements in the literature, highlighting the practical implications of fractional calculus in Cosmology and the potential of our theory to alleviate the constant tension of the Hubble, offering hope for future research in this area.

Author contributions

Conceptualization, B. M., B. D., A.D.M., and G.L.; methodology, G.L.; software, B. M., B. D., A.D.M., G.L., E.G. and J.M.; validation, B. M., B. D., A.D.M., G.L. E.G. and J.M.; formal analysis, B. M., B. D., A.D.M., G.L., E.G. and J.M.; investigation, B. M., B. D., A.D.M., G.L. E.G. and J.M.; resources, G.L. and J.M.; writing—original draft preparation, G.L.; writing—review and editing, G.L.; visualization, B. M., B. D., A.D.M., G.L. E.G. and J.M.; supervision, G.L., B.D., and A.M.; project administration, G.L. J.M., and B. M., B. D.; funding acquisition, B. M., B. D., A.D.M., G.L, E.G. and J.M. All authors have read and agreed to the published version of the manuscript.

Funding

B.M., G.L., J.M., and A.D.M acknowledge the financial support of Agencia Nacional de Investigación y Desarrollo (ANID), Chile, through Proyecto Fondecyt Regular 2024, Folio 1240514, Etapa 2024. G.L. was also funded by Vicerrectoría de Investigación y Desarrollo Tecnológico (VRIDT) at Universidad Católica del Norte (UCN) through Resolución VRIDT N°026/2023, Resolución VRIDT N°027/2023, Proyecto de Investigación Pro Fondecyt 2023 (Resolución VRIDT N°076/2023) and Resolución VRIDT N°09/2024. He also acknowledges the scientific support of Núcleo de Investigación Geometría Diferencial y Aplicaciones (Resolución VRIDT N°096/2022). A.D.M. was also supported by Agencia Nacional de Investigación y Desarrollo - ANID Subdirección de Capital Humano/Doctorado Nacional/año 2020 folio 21200837, Gastos operacionales proyecto de Tesis/2022 folio 242220121 and VRIDT-UCN. E.G. was funded by Vicerrectoría de Investigación y Desarrollo Tecnológico (VRIDT) at Universidad Católica del Norte (UCN) through Proyecto de Investigación Pro Fondecyt 2023, Resolución VRIDT N°076/2023.

Data availability

No new data were created or analyzed in this study. Data sharing is not applicable to this article.

Acknowledgments

We are thankful for the support of Núcleo de Investigación Geometría Diferencial y Aplicaciones, Resolución VRIDT N°096/2022. E.G. acknowledges the scientific support of Núcleo de Investigación No. 7 UCN-VRIDT 076/2020, Núcleo de Modelación y Simulación Científica (NMSC).

Conflicts of interest

We declare no conflict of interest. The funders had no role in the design of the study; in the collection, analyses, or interpretation of data; in the writing of the manuscript; or in the decision to publish the results.

Appendix A: Variational equations

We start with an action defined as [162]

$$S = \frac{1}{\Gamma(\mu)} \int_0^\tau \mathcal{L}(\theta, q_i(\theta), \dot{q}_i(\theta), \ddot{q}_i(\theta)) (\tau - \theta)^{\mu-1} d\theta, \quad (\text{A1})$$

where $\dot{q}_i(\theta)$, $\ddot{q}_i(\theta)$ means integer order derivatives with respect to the argument θ .

To obtain the equations of motion of the fields, we do the infinitesimal transformation of the fields

$$q_i \mapsto q_i + \delta q_i, \delta \mathcal{L} = \mathcal{L}(q_i + \delta q_i) - \mathcal{L}(q_i). \quad (\text{A2})$$

Then, we write the variation of the action:

$$\begin{aligned} \delta S &= \frac{1}{\Gamma(\mu)} \int_0^\tau [(\delta \mathcal{L})(\tau - \theta)^{\mu-1} + \mathcal{L} \delta((\tau - \theta)^{\mu-1})] d\theta \\ &= \frac{1}{\Gamma(\mu)} \int_0^\tau \left[\left(\frac{\partial \mathcal{L}}{\partial q_i} \delta q_i + \frac{\partial \mathcal{L}}{\partial \dot{q}_i} \delta \dot{q}_i + \frac{\partial \mathcal{L}}{\partial \ddot{q}_i} \delta \ddot{q}_i \right) (\tau - \theta)^{\mu-1} \right] d\theta. \end{aligned} \quad (\text{A3})$$

We can integrate by parts:

$$\int_0^\tau \frac{\partial \mathcal{L}}{\partial \dot{q}_i} (\tau - \theta)^{\mu-1} \delta \dot{q}_i d\theta = \frac{\partial \mathcal{L}}{\partial \dot{q}_i} (\tau - \theta)^{\mu-1} \delta q_i \Big|_0^\tau - \int_0^\tau \frac{d}{d\theta} \left[\frac{\partial \mathcal{L}}{\partial \dot{q}_i} (\tau - \theta)^{\mu-1} \right] \delta q_i d\theta, \quad (\text{A4})$$

$$\begin{aligned} \int_0^\tau \frac{\partial \mathcal{L}}{\partial \ddot{q}_i} (\tau - \theta)^{\mu-1} \delta \ddot{q}_i d\theta &= \frac{\partial \mathcal{L}}{\partial \ddot{q}_i} (\tau - \theta)^{\mu-1} \delta \dot{q}_i \Big|_0^\tau - \int_0^\tau \frac{d}{d\theta} \left[\frac{\partial \mathcal{L}}{\partial \ddot{q}_i} (\tau - \theta)^{\mu-1} \right] \delta \dot{q}_i d\theta \\ &= -\frac{d}{d\theta} \left[\frac{\partial \mathcal{L}}{\partial \ddot{q}_i} (\tau - \theta)^{\mu-1} \right] \delta q_i \Big|_0^\tau + \frac{\partial \mathcal{L}}{\partial \ddot{q}_i} (\tau - \theta)^{\mu-1} \delta \dot{q}_i \Big|_0^\tau \\ &\quad + \int_0^\tau \frac{d^2}{d\theta^2} \left[\frac{\partial \mathcal{L}}{\partial \ddot{q}_i} (\tau - \theta)^{\mu-1} \right] \delta q_i d\theta. \end{aligned} \quad (\text{A5})$$

Therefore, the variation of the action can be written as

$$\begin{aligned} \delta S &= \frac{1}{\Gamma(\mu)} \int_0^\tau \left\{ \frac{\partial \mathcal{L}}{\partial q_i} (\tau - \theta)^{\mu-1} - \frac{d}{d\theta} \left[\frac{\partial \mathcal{L}}{\partial \dot{q}_i} (\tau - \theta)^{\mu-1} \right] + \frac{d^2}{d\theta^2} \left[\frac{\partial \mathcal{L}}{\partial \ddot{q}_i} (\tau - \theta)^{\mu-1} \right] \right\} \delta q_i d\theta \\ &\quad + \left\{ \frac{\partial \mathcal{L}}{\partial \dot{q}_i} (\tau - \theta)^{\mu-1} - \frac{d}{d\theta} \left[\frac{\partial \mathcal{L}}{\partial \ddot{q}_i} (\tau - \theta)^{\mu-1} \right] \right\} \delta q_i \Big|_0^\tau + \frac{\partial \mathcal{L}}{\partial \ddot{q}_i} (\tau - \theta)^{\mu-1} \delta \dot{q}_i \Big|_0^\tau. \end{aligned} \quad (\text{A6})$$

Then, assuming that δq_i is zero at the lower end, $\delta q_i(0) = 0$, we have the equations of motion:

$$\frac{\partial \mathcal{L}}{\partial q_i} (\tau - \theta)^{\mu-1} - \frac{d}{d\theta} \left[\frac{\partial \mathcal{L}}{\partial \dot{q}_i} (\tau - \theta)^{\mu-1} \right] + \frac{d^2}{d\theta^2} \left[\frac{\partial \mathcal{L}}{\partial \ddot{q}_i} (\tau - \theta)^{\mu-1} \right] = 0. \quad (\text{A7})$$

For the more general case where the Lagrangian depends on derivatives of up to order n of the generalized coordinates, the same procedure can be used to show that, through successive integration by parts, alternating signs emerge and the derivatives of order k are as follows:

$$\sum_{k=0}^n (-1)^k \frac{d^k}{d\theta^k} \left[\frac{\partial \mathcal{L}}{\partial (q_i^{(k)})} (\tau - \theta)^{\mu-1} \right] = 0. \quad (\text{A8})$$

In our particular case, $n = 2$ for the generalized coordinate q_i .

Appendix B: Stability analysis of power-law solutions

In general, when we have an ordinary differential equation

$$\mathcal{F} \left(t, \psi(t), \dot{\psi}(t), \ddot{\psi}(t), \dots \right) \equiv 0, \quad (\text{B1})$$

where t is the independent variable and $\psi(t)$ is the dependent variable; we can provide the analysis of the stability of the solution $\psi_s(t)$ in the interval $0 < t < \infty$ using similar methods as in [159, 160] and [161]. Defining the new time variable

$$t = e^\tau, \quad -\infty < \tau < \infty, \quad (\text{B2})$$

such that $t \rightarrow 0$ as $\tau \rightarrow -\infty$ and $t \rightarrow \infty$ as $\tau \rightarrow \infty$, as well as the ratio

$$u(\tau) = \frac{\psi(\tau)}{\psi_s(\tau)}, \quad (\text{B3})$$

where $\psi(\tau) = \psi(e^\tau)$ and $\psi_s(\tau) = \psi_s(e^\tau)$ given. Notice that evaluated at $\psi_s(\tau)$ we have $u = 1$, therefore, defining $\varepsilon = \frac{\psi(\tau)}{\psi_s(\tau)} - 1$ the solution is shifted to $\varepsilon = 0$. Let

$$\psi' \equiv \frac{d\psi}{d\tau}, \quad (\text{B4})$$

then,

$$\dot{\psi} = \frac{d\tau}{dt} \psi' = e^{-\tau} \psi', \quad \ddot{\psi} = e^{-2\tau} (\psi'' - \psi'). \quad (\text{B5})$$

Therefore, the equation (B1) becomes

$$\mathcal{G}(\tau, u(\tau), u'(\tau), u''(\tau), \dots) \equiv 0. \quad (\text{B6})$$

According to (59), $\psi(t)$ satisfies

$$\ddot{\psi} = c_1 + c_2 \frac{\psi}{t^2} + c_3 \frac{\dot{\psi}}{t}, \quad (\text{B7})$$

where c_1 , c_2 , and c_3 are the constants. Additionally, given the solution found for the exponential potential, (46), the critical solution (63) can be expressed as:

$$\psi_c(t) = c_4 t^2, \quad (\text{B8})$$

where c_4 is also a constant.

Thus, replacing $\ddot{\psi}$, $\dot{\psi}$, and t , (B7) becomes

$$e^{-2\tau} [\psi''(\tau) - \psi'(\tau)] = c_1 + c_2 e^{-2\tau} \psi(\tau) + c_3 e^{-2\tau} \psi'(\tau), \quad (\text{B9})$$

That is,

$$\psi''(\tau) = c_1 e^{2\tau} + c_2 \psi(\tau) + (c_3 + 1) \psi'(\tau). \quad (\text{B10})$$

Using the definition of ε , we see that

$$\begin{aligned} \psi(\tau) &= (\varepsilon(\tau) + 1) \psi_c(\tau), \\ \psi'(\tau) &= \varepsilon'(\tau) \psi_c(\tau) + (\varepsilon(\tau) + 1) \psi_c'(\tau), \\ \psi''(\tau) &= \varepsilon''(\tau) \psi_c(\tau) + 2\varepsilon'(\tau) \psi_c'(\tau) + (\varepsilon(\tau) + 1) \psi_c''(\tau). \end{aligned} \quad (\text{B11})$$

Therefore,

$$\varepsilon''\psi_c + 2\varepsilon'\psi'_c + (\varepsilon + 1)\psi''_c = c_1e^{2\tau} + c_2(\varepsilon + 1)\psi_c + (c_3 + 1)[\varepsilon'\psi_c + (\varepsilon + 1)\psi'_c]. \quad (\text{B12})$$

Equation (B12) can be written as

$$\varepsilon''\psi_c + 2\varepsilon'\psi'_c + \varepsilon\psi''_c + \underbrace{[\psi''_c - c_1e^{2\tau} - c_2\psi_c - (c_3 + 1)\psi'_c]}_{=0, \psi_c(\tau) \text{ satisfies (B10)}} = c_2\varepsilon\psi_c + (c_3 + 1)(\varepsilon'\psi_c + \varepsilon\psi'_c) \quad (\text{B13})$$

Due to $\psi_c(\tau)$ being a non-trivial particular solution of equation (B10), the term inside squared brackets on the left-hand side of (B13) is zero. After simplification, we acquire

$$\varepsilon'' + 2\varepsilon'\frac{\psi'_c}{\psi_c} + \varepsilon\frac{\psi''_c}{\psi_c} = c_2\varepsilon + (c_3 + 1)\left(\varepsilon' + \varepsilon\frac{\psi'_c}{\psi_c}\right). \quad (\text{B14})$$

Note that

$$\psi_c(\tau) = c_4e^{2\tau}, \psi'_c(\tau) = 2c_4e^{2\tau}, \psi''_c(\tau) = 4c_4e^{2\tau}. \quad (\text{B15})$$

Therefore,

$$\frac{\psi'_c}{\psi_c} = 2, \quad \frac{\psi''_c}{\psi_c} = 4. \quad (\text{B16})$$

Hence, by reducing terms, we have

$$\varepsilon'' = \varepsilon'(c_3 - 3) + \varepsilon(c_2 + 2c_3 - 2). \quad (\text{B17})$$

Defining $v = \varepsilon'$, we have the linear system

$$\varepsilon' = v, \quad v' = \varepsilon(c_2 + 2c_3 - 2) + v(c_3 - 3), \quad (\text{B18})$$

that was investigated using dynamical systems tools in §4 for the choice of the constants:

$$c_1 = \frac{1}{32}[m(-4\mu + (\mu - 2)(\mu - 1)m + 18) - 12], c_2 = \frac{m[\mu(-\mu m + m + 4) - 22] + 12}{m^2},$$

$$c_3 = 2\left(\mu - \frac{2}{m}\right), c_4 = \frac{1}{96}m^2\left(\frac{2m(3\lambda^2 + m)}{\lambda^2[(\mu - 6)m + 2]} + 3\right).$$

[1] A. G. Riess, A. V. Filippenko, P. Challis, A. Clocchiatti, A. Diercks, et al., The Astronomical Journal **116**, 1009 (1998), URL <http://stacks.iop.org/1538-3881/116/i=3/a=1009>.

- [2] N. Aghanim et al. (Planck), *Astron. Astrophys.* **641**, A6 (2020), [Erratum: *Astron. Astrophys.* 652, C4 (2021)], 1807.06209.
- [3] Y. B. Zeldovich, *Soviet Physics Uspekhi* **11** (1968).
- [4] S. Weinberg, *Reviews of Modern Physics* **61** (1989).
- [5] S. M. Carroll, *Living Rev. Rel.* **4**, 1 (2001), astro-ph/0004075.
- [6] S. M. M. Rasouli, A. H. Ziaie, J. Marto, and P. V. Moniz, *Phys. Rev. D* **89**, 044028 (2014), 1309.6622.
- [7] S. Jalalzadeh, S. M. M. Rasouli, and P. V. Moniz, *Phys. Rev. D* **90**, 023541 (2014), 1403.1419.
- [8] S. M. M. Rasouli, M. Farhoudi, and P. Vargas Moniz, *Class. Quant. Grav.* **31**, 115002 (2014), 1405.0229.
- [9] S. M. M. Rasouli and P. Vargas Moniz, *Phys. Rev. D* **90**, 083533 (2014), 1411.1346.
- [10] S. M. M. Rasouli, A. H. Ziaie, S. Jalalzadeh, and P. V. Moniz, *Annals Phys.* **375**, 154 (2016), 1608.05958.
- [11] S. M. M. Rasouli and P. Vargas Moniz, *Odessa Astron. Pub.* **29**, 19 (2016), 1611.00085.
- [12] S. Jalalzadeh, A. J. S. Capistrano, and P. V. Moniz, *Phys. Dark Univ.* **18**, 55 (2017), 1709.09923.
- [13] A. Melchiorri, L. Mersini-Houghton, C. J. Odman, and M. Trodden, *Phys. Rev. D* **68**, 043509 (2003), astro-ph/0211522.
- [14] A. Vikman, *Phys. Rev. D* **71**, 023515 (2005), astro-ph/0407107.
- [15] G. Leon, Y. Leyva, E. N. Saridakis, O. Martin, and R. Cardenas, *Falsifying Field-based Dark Energy Models* (2009), 0912.0542.
- [16] S. Nesseris and L. Perivolaropoulos, *JCAP* **01**, 018 (2007), astro-ph/0610092.
- [17] B. Feng, X.-L. Wang, and X.-M. Zhang, *Phys. Lett. B* **607**, 35 (2005), astro-ph/0404224.
- [18] H. Wei and R.-G. Cai, *Phys. Rev. D* **72**, 123507 (2005), astro-ph/0509328.
- [19] H. Wei and R.-G. Cai, *Phys. Lett. B* **634**, 9 (2006), astro-ph/0512018.
- [20] H. Wei, R.-G. Cai, and D.-F. Zeng, *Class. Quant. Grav.* **22**, 3189 (2005), hep-th/0501160.
- [21] Z.-K. Guo, Y.-S. Piao, X.-M. Zhang, and Y.-Z. Zhang, *Phys. Lett. B* **608**, 177 (2005), astro-ph/0410654.
- [22] X.-F. Zhang, H. Li, Y.-S. Piao, and X.-M. Zhang, *Mod. Phys. Lett. A* **21**, 231 (2006), astro-ph/0501652.
- [23] B. Feng, M. Li, Y.-S. Piao, and X. Zhang, *Phys. Lett. B* **634**, 101 (2006), astro-ph/0407432.

- [24] X. Wu (CDF), PoS **HEP2005**, 155 (2006).
- [25] J.-Q. Xia, B. Feng, and X.-M. Zhang, Mod. Phys. Lett. A **20**, 2409 (2005), astro-ph/0411501.
- [26] G.-B. Zhao, J.-Q. Xia, M. Li, B. Feng, and X. Zhang, Phys. Rev. D **72**, 123515 (2005), astro-ph/0507482.
- [27] X. Zhang, Commun. Theor. Phys. **44**, 762 (2005).
- [28] X. Zhang, Int. J. Mod. Phys. D **14**, 1597 (2005), astro-ph/0504586.
- [29] X. Zhang and F.-Q. Wu, Phys. Rev. D **72**, 043524 (2005), astro-ph/0506310.
- [30] X. Zhang, Phys. Rev. D **74**, 103505 (2006), astro-ph/0609699.
- [31] R. Lazkoz and G. Leon, Phys. Lett. B **638**, 303 (2006), astro-ph/0602590.
- [32] R. Lazkoz, G. Leon, and I. Quiros, Phys. Lett. B **649**, 103 (2007), astro-ph/0701353.
- [33] H. Mohseni Sadjadi and M. Alimohammadi, Phys. Rev. D **74**, 043506 (2006), gr-qc/0605143.
- [34] M. Alimohammadi and H. M. Sadjadi, Phys. Lett. B **648**, 113 (2007), gr-qc/0608016.
- [35] E. Elizalde, S. Nojiri, S. D. Odintsov, D. Saez-Gomez, and V. Faraoni, Phys. Rev. D **77**, 106005 (2008), 0803.1311.
- [36] Y.-F. Cai, E. N. Saridakis, M. R. Setare, and J.-Q. Xia, Phys. Rept. **493**, 1 (2010), 0909.2776.
- [37] G. Leon, Y. Leyva, and J. Socorro, Phys. Lett. B **732**, 285 (2014), 1208.0061.
- [38] G. Leon, A. Paliathanasis, and J. L. Morales-Martínez, Eur. Phys. J. C **78**, 753 (2018), 1808.05634.
- [39] J. Tot, B. Yildirim, A. Coley, and G. Leon, Phys. Dark Univ. **39**, 101155 (2023), 2204.06538.
- [40] G. Leon, A. Coley, A. Paliathanasis, J. Tot, and B. Yildirim, Phys. Dark Univ. **45**, 101503 (2024), 2308.02470.
- [41] A. Paliathanasis, Class. Quant. Grav. **37**, 195014 (2020), 2003.05342.
- [42] A. Paliathanasis and G. Leon, Class. Quant. Grav. **38**, 075013 (2021), 2009.12874.
- [43] R. Curbelo, T. Gonzalez, G. Leon, and I. Quiros, Class. Quant. Grav. **23**, 1585 (2006), astro-ph/0502141.
- [44] E. Elizalde, S. Nojiri, and S. D. Odintsov, Phys. Rev. D **70**, 043539 (2004), hep-th/0405034.
- [45] P. S. Apostolopoulos and N. Tetradis, Phys. Rev. D **74**, 064021 (2006), hep-th/0604014.
- [46] K. Bamba, S. Nojiri, and S. D. Odintsov, Phys. Rev. D **77**, 123532 (2008), 0803.3384.
- [47] K. Bamba, C.-Q. Geng, S. Nojiri, and S. D. Odintsov, Phys. Rev. D **79**, 083014 (2009), 0810.4296.
- [48] M. R. Setare and E. N. Saridakis, JCAP **03**, 002 (2009), 0811.4253.

- [49] S. M. Carroll, A. De Felice, V. Duvvuri, D. A. Easson, M. Trodden, and M. S. Turner, *Phys. Rev. D* **71**, 063513 (2005), astro-ph/0410031.
- [50] S. M. Carroll, V. Duvvuri, M. Trodden, and M. S. Turner, *Phys. Rev. D* **70**, 043528 (2004), astro-ph/0306438.
- [51] S. Capozziello, V. F. Cardone, S. Carloni, and A. Troisi, *Int. J. Mod. Phys. D* **12**, 1969 (2003), astro-ph/0307018.
- [52] S. Capozziello, S. Carloni, and A. Troisi, *Recent Res. Dev. Astron. Astrophys.* **1**, 625 (2003), astro-ph/0303041.
- [53] S. Nojiri and S. D. Odintsov, *eConf* **C0602061**, 06 (2006), hep-th/0601213.
- [54] S. Capozziello and M. Francaviglia, *Gen. Rel. Grav.* **40**, 357 (2008), 0706.1146.
- [55] D. Wands, *Class. Quant. Grav.* **11**, 269 (1994), gr-qc/9307034.
- [56] S. Capozziello, A. Stabile, and A. Troisi, *Phys. Lett. B* **686**, 79 (2010), 1002.1364.
- [57] S. Capozziello, M. De Laurentis, M. Francaviglia, and S. Mercadante, *AIP Conf. Proc.* **1241**, 844 (2010), 0911.2159.
- [58] S. Capozziello, M. De Laurentis, and V. Faraoni, *Open Astron. J.* **3**, 49 (2010), 0909.4672.
- [59] S. Capozziello, *PoS QG-PH*, 015 (2007).
- [60] S. Capozziello, E. Elizalde, S. Nojiri, and S. D. Odintsov, *Phys. Lett. B* **671**, 193 (2009), 0809.1535.
- [61] S. Capozziello, *Int. J. Mod. Phys. D* **11**, 483 (2002), gr-qc/0201033.
- [62] V. Faraoni, *Phys. Rev. D* **72**, 124005 (2005), gr-qc/0511094.
- [63] M. L. Ruggiero and L. Iorio, *JCAP* **01**, 010 (2007), gr-qc/0607093.
- [64] A. de la Cruz-Dombriz and A. Dobado, *Phys. Rev. D* **74**, 087501 (2006), gr-qc/0607118.
- [65] N. J. Poplawski, *Phys. Rev. D* **74**, 084032 (2006), gr-qc/0607124.
- [66] A. W. Brookfield, C. van de Bruck, and L. M. H. Hall, *Phys. Rev. D* **74**, 064028 (2006), hep-th/0608015.
- [67] Y.-S. Song, W. Hu, and I. Sawicki, *Phys. Rev. D* **75**, 044004 (2007), astro-ph/0610532.
- [68] B. Li, K. C. Chan, and M. C. Chu, *Phys. Rev. D* **76**, 024002 (2007), astro-ph/0610794.
- [69] T. P. Sotiriou, *Class. Quant. Grav.* **23**, 5117 (2006), gr-qc/0604028.
- [70] O. Bertolami and M. Carvalho Sequeira, *AIP Conf. Proc.* **1241**, 729 (2010), 0910.3876.
- [71] O. Bertolami and M. C. Sequeira, *Phys. Rev. D* **79**, 104010 (2009), 0903.4540.
- [72] O. Bertolami, C. G. Boehmer, T. Harko, and F. S. N. Lobo, *Phys. Rev. D* **75**, 104016 (2007),

- 0704.1733.
- [73] F. Briscese, E. Elizalde, S. Nojiri, and S. D. Odintsov, *Phys. Lett. B* **646**, 105 (2007), hep-th/0612220.
- [74] G. Leon and E. N. Saridakis, *Class. Quant. Grav.* **28**, 065008 (2011), 1007.3956.
- [75] G. Leon and E. N. Saridakis, *JCAP* **11**, 006 (2009), 0909.3571.
- [76] J. Bellorin, C. Borquez, and B. Droguett, *Phys. Rev. D* **109**, 084007 (2024), 2312.16327.
- [77] J. Bellorin, C. Borquez, and B. Droguett, *Renormalization of the nonprojectable Horava theory* (2024), 2405.04708.
- [78] C. R. Fadrugas and G. Leon, *Class. Quant. Grav.* **31**, 195011 (2014), 1405.2465.
- [79] G. Leon, *Class. Quant. Grav.* **26**, 035008 (2009), 0812.1013.
- [80] G. Leon and F. O. F. Silva, *Class. Quant. Grav.* **37**, 245005 (2020), 2007.11140.
- [81] G. Leon and F. O. F. Silva, *Class. Quant. Grav.* **38**, 015004 (2021), 2007.11990.
- [82] G. Leon and E. N. Saridakis, *Phys. Lett. B* **693**, 1 (2010), 0904.1577.
- [83] V. E. Tarasov, *International Journal of Modern Physics B* **27** (2013), ISSN 0217-9792.
- [84] C. A. Monje, Y. Q. Chen, B. M. Vinagre, D. Xue, and V. Feliu-Batlle, *Fractional-order Systems and Controls: Fundamentals and Applications*, Advances in Industrial Control (Springer London, 2010), ISBN 9781849963350, URL <https://books.google.cl/books?id=c4fv9WeCiEwC>.
- [85] B. Bandyopadhyay and S. Kamal, *Stabilization and Control of Fractional Order Systems: A Sliding Mode Approach*, Lecture Notes in Electrical Engineering (Springer International Publishing, 2014), ISBN 9783319086217, URL <https://books.google.cl/books?id=GtgkBAAAQBAJ>.
- [86] F. Padula and A. Visioli, *Advances in Robust Fractional Control* (Springer International Publishing, 2014), ISBN 9783319109305, URL <https://books.google.cl/books?id=qGSSBAAAQBAJ>.
- [87] R. Herrmann, *Fractional Calculus: An Introduction For Physicists (2nd Edition)* (World Scientific Publishing Company, 2014), ISBN 9789814551090, URL <https://books.google.cl/books?id=60S7CgAAQBAJ>.
- [88] V. E. Tarasov, *Applications in Physics, Part A*, De Gruyter Reference (De Gruyter, 2019), ISBN 9783110571707, URL <https://books.google.cl/books?id=MXacDwAAQBAJ>.
- [89] J. Klafter, S. C. Lim, and R. Metzler, *Fractional Dynamics: Recent Advances* (World Scientific, 2012), ISBN 9789814340588, URL <https://books.google.cl/books?id=2Q5qDQAAQBAJ>.
- [90] A. B. Malinowska, T. Odziejewicz, and D. F. M. Torres, *Advanced Methods in the Fractional*

- Calculus of Variations*, Springer briefs in applied sciences and technology (Springer International Publishing, 2015), ISBN 9783319147574, URL <https://books.google.cl/books?id=qDjkzQEACAAJ>.
- [91] C. F. Lorenzo and T. T. Hartley, *The Fractional Trigonometry: With Applications to Fractional Differential Equations and Science* (Wiley, 2016), ISBN 9781119139423, URL <https://books.google.cl/books?id=LdyADQAAQBAJ>.
- [92] S. C. Lim, *Physica A* **363**, 269 (2006).
- [93] S. C. Lim and C. H. E. V. E. T. (ed.), *Fractional quantum fields* (De Gruyter, 2019), pp. 237–256.
- [94] A. R. El-Nabulsi, *Indian J. Phys.* **87**, 195 (2013).
- [95] A. R. El-Nabulsi, *Indian J. Phys.* **87**, 835 (2013).
- [96] P. V. Moniz and S. Jalalzadeh, *Mathematics* **8**, 313 (2020), 2003.01070.
- [97] S. M. M. Rasouli, S. Jalalzadeh, and P. V. Moniz, *Mod. Phys. Lett. A* **36**, 2140005 (2021), 2101.03065.
- [98] P. V. Moniz and S. Jalalzadeh, *Challenging Routes in Quantum Cosmology* (World Scientific Publishing, Singapore, 2020), ISBN 978-981-4415-06-4.
- [99] G. Calcagni and S. Kuroyanagi, *JCAP* **03**, 019 (2021), 2012.00170.
- [100] S. I. Vacaru, *Int. J. Theor. Phys.* **51**, 1338 (2012), 1004.0628.
- [101] S. Jalalzadeh, F. R. da Silva, and P. V. Moniz, *Eur. Phys. J. C* **81**, 632 (2021), 2107.04789.
- [102] R. A. El-Nabulsi, *Rom. Rep. Phys.* **59**, 763 (2007).
- [103] A. R. El-Nabulsi, *Int. J. Geom. Meth. Mod. Phys.* **6**, 25 (2009).
- [104] R. A. EL-Nabulsi, *Chaos Solitons Fractals* **41**, 2262 (2009).
- [105] S. I. Vacaru, *Chaos Solitons Fractals* **45**, 1266 (2012), 1004.0625.
- [106] M. Jamil, D. Momeni, and M. A. Rashid, *J. Phys. Conf. Ser.* **354**, 012008 (2012), 1106.2974.
- [107] U. Debnath, M. Jamil, and S. Chattopadhyay, *International Journal of Theoretical Physics* **51**, 812 (2012).
- [108] U. Debnath, S. Chattopadhyay, and M. Jamil, *Journal of Theoretical and Applied Physics* **7**, 25 (2013).
- [109] V. K. Shchigolev, *Eur. Phys. J. Plus* **131**, 256 (2016), 1512.04113.
- [110] E.-N. A. Rami, *Eur. Phys. J. Plus* **130**, 102 (2015).
- [111] A. Giusti, *Phys. Rev. D* **101**, 124029 (2020), 2002.07133.

- [112] G. Calcagni, Phys. Rev. Lett. **104**, 251301 (2010), 0912.3142.
- [113] G. Calcagni, JHEP **03**, 120 (2010), 1001.0571.
- [114] G. Calcagni, JCAP **12**, 041 (2013), 1307.6382.
- [115] G. Calcagni, Class. Quant. Grav. **38**, 165005 (2021), [Erratum: Class.Quant.Grav. 38, 169601 (2021)], 2106.15430.
- [116] G. Calcagni, Classical and Quantum Gravity **38**, 165006 (2021), URL <https://doi.org/10.1088/1361-6382/ac103c>.
- [117] G. Calcagni and A. De Felice, Phys. Rev. D **102**, 103529 (2020), 2004.02896.
- [118] G. Calcagni, S. Kuroyanagi, S. Marsat, M. Sakellariadou, N. Tamanini, and G. Tasinato, JCAP **10**, 012 (2019), 1907.02489.
- [119] G. Calcagni, S. Kuroyanagi, and S. Tsujikawa, JCAP **08**, 039 (2016), 1606.08449.
- [120] S. I. Vacaru, Int. J. Theor. Phys. **49**, 2753 (2010), 1003.0043.
- [121] M. D. Roberts, SOP Trans. Theor. Phys. **1**, 310 (2014), 0909.1171.
- [122] V. K. Shchigolev, Commun. Theor. Phys. **56**, 389 (2011), 1011.3304.
- [123] V. K. Shchigolev, Discontinuity Nonlinearity and Complexity **2**, 115 (2013), 1208.3454.
- [124] V. K. Shchigolev, Mod. Phys. Lett. A **28**, 1350056 (2013), 1301.7198.
- [125] V. K. Shchigolev, Mod. Phys. Lett. A **36**, 2130014 (2021), 2104.12610.
- [126] S. Jalalzadeh, E. W. O. Costa, and P. V. Moniz, Phys. Rev. D **105**, L121901 (2022), 2206.07818.
- [127] M. A. García-Aspeitia, G. Fernandez-Anaya, A. Hernández-Almada, G. Leon, and J. Magaña, Mon. Not. Roy. Astron. Soc. **517**, 4813 (2022), 2207.00878.
- [128] R. G. Landim, Phys. Rev. D **104**, 103508 (2021), 2106.15415.
- [129] R. G. Landim, Phys. Rev. D **103**, 083511 (2021), 2101.05072.
- [130] B. Micolta-Riascos, A. D. Millano, G. Leon, C. Erices, and A. Paliathanasis, Fractal and Fractional **7** (2023), ISSN 2504-3110, URL <https://www.mdpi.com/2504-3110/7/2/149>.
- [131] E. González, G. Leon, and G. Fernandez-Anaya, Fractal Fract. **7**, 368 (2023), 2303.16409.
- [132] G. Leon Torres, M. A. García-Aspeitia, G. Fernandez-Anaya, A. Hernández-Almada, J. Magaña, and E. González, PoS **CORFU2022**, 248 (2023), 2304.14465.
- [133] A. Hernández-Almada, G. Leon, J. Magaña, M. A. García-Aspeitia, and V. Motta, Mon. Not. Roy. Astron. Soc. **497**, 1590 (2020), 2002.12881.
- [134] G. Leon, J. Magaña, A. Hernández-Almada, M. A. García-Aspeitia, T. Verdugo, and V. Motta, JCAP **12**, 032 (2021), 2108.10998.

- [135] A. Hernández-Almada, G. Leon, J. Magaña, M. A. García-Aspeitia, V. Motta, E. N. Saridakis, K. Yesmakhanova, and A. D. Millano, *Mon. Not. Roy. Astron. Soc.* **512**, 5122 (2022), 2112.04615.
- [136] A. Hernández-Almada, G. Leon, J. Magaña, M. A. García-Aspeitia, V. Motta, E. N. Saridakis, and K. Yesmakhanova, *Mon. Not. Roy. Astron. Soc.* **511**, 4147 (2022), 2111.00558.
- [137] J. M. Armaleo, J. Osorio Morales, and O. Santillan, *Eur. Phys. J. C* **78**, 85 (2018), 1711.09484.
- [138] S. Nojiri, S. D. Odintsov, and M. Sasaki, *Phys. Rev. D* **71**, 123509 (2005), hep-th/0504052.
- [139] S. Nojiri, S. D. Odintsov, and M. Sami, *Phys. Rev. D* **74**, 046004 (2006), hep-th/0605039.
- [140] G. Cognola, E. Elizalde, S. Nojiri, S. Odintsov, and S. Zerbini, *Phys. Rev. D* **75**, 086002 (2007), hep-th/0611198.
- [141] S. Nojiri, S. D. Odintsov, and P. V. Tretyakov, *Phys. Lett. B* **651**, 224 (2007), 0704.2520.
- [142] T. Padmanabhan and D. Kothawala, *Phys. Rept.* **531**, 115 (2013), 1302.2151.
- [143] S. Chakraborty, T. Paul, and S. SenGupta, *Phys. Rev. D* **98**, 083539 (2018), 1804.03004.
- [144] I. V. Fomin, *Phys. Part. Nucl.* **49**, 525 (2018).
- [145] P. Kanti, R. Gannouji, and N. Dadhich, *Phys. Rev. D* **92**, 041302 (2015), 1503.01579.
- [146] G. Hikmawan, J. Soda, A. Suroso, and F. P. Zen, *Phys. Rev. D* **93**, 068301 (2016), 1512.00222.
- [147] M. Motaharfar and H. R. Sepangi, *Eur. Phys. J. C* **76**, 646 (2016), 1604.00453.
- [148] N. Rashidi and K. Nozari, *Astrophys. J.* **890**, 58 (2020), 2001.07012.
- [149] A. D. Millano, G. Leon, and A. Paliathanasis, *Mathematics* **11**, 1408 (2023), 2302.09371.
- [150] A. D. Millano, G. Leon, and A. Paliathanasis, *Phys. Rev. D* **108**, 023519 (2023), 2304.08659.
- [151] E. Barrientos, S. Mendoza, and P. Padilla, *Symmetry* **13**, 174 (2021), 2012.03446.
- [152] D. Baleanu and S. Muslih, *Lagrangian formulation of classical fields within riemann-liouville fractional derivatives* (2005).
- [153] P. Agrawal, O, *Fractional variational calculus in terms of riesz fractional derivatives* (2007).
- [154] A. El-Nabulsi, R. and F. Torres, D, *Fractional action-like variational problems* (2008).
- [155] D. Baleanu and J. Trujillo, *A new method of finding the fractional euler-lagrange and hamilton equations within caputo fractional derivatives* (2010).
- [156] T. Odziejewicz, A. Malinowska, and D. Torres, *Variable order fractional variational calculus for double integrals* (2013).
- [157] T. Odziejewicz, A. Malinowska, and D. Torres, *Noether's theorem for fractional variational problems of variable order* (2013).

- [158] T. Odziejewicz, A. Malinowska, and D. Torres, *A generalized fractional calculus of variations* (2013).
- [159] B. Ratra and P. J. E. Peebles, *Phys. Rev. D* **37**, 3406 (1988).
- [160] A. R. Liddle and R. J. Scherrer, *Phys. Rev. D* **59**, 023509 (1999), astro-ph/9809272.
- [161] J.-P. Uzan, *Phys. Rev. D* **59**, 123510 (1999), gr-qc/9903004.
- [162] D. Frederico, G.A.S.F.; Torres, *WSEAS Trans. Math.* **7**, 6–11 (2008).
- [163] L. Perko, *Differential equations and dynamical systems, third edition* (Springer-Verlag, 2001).
- [164] J. Goodman and J. Weare, *Commun. Appl. Math. Comput. Sci.* **5**, 65 (2010).
- [165] D. Foreman-Mackey, D. W. Hogg, D. Lang, and J. Goodman, *Publ. Astron. Soc. Pac.* **125**, 306 (2013), 1202.3665.
- [166] S. Capozziello, R. D’Agostino, and O. Luongo, *Mon. Not. Roy. Astron. Soc.* **476**, 3924 (2018), 1712.04380.
- [167] R. Jimenez and A. Loeb, *Astrophys. J.* **573**, 37 (2002), astro-ph/0106145.
- [168] D. Brout et al., *Astrophys. J.* **938**, 110 (2022), 2202.04077.
- [169] R. Tripp, *Astron. Astrophys.* **331**, 815 (1998).
- [170] R. Kessler and D. Scolnic, *Astrophys. J.* **836**, 56 (2017), 1610.04677.
- [171] A. G. Riess et al., *Astrophys. J. Lett.* **934**, L7 (2022), 2112.04510.
- [172] T. Treu and P. J. Marshall, *Astron. Astrophys. Rev.* **24**, 11 (2016), 1605.05333.
- [173] K. C. Wong et al., *Mon. Not. Roy. Astron. Soc.* **498**, 1420 (2020), 1907.04869.
- [174] I. Jee, S. H. Suyu, E. Komatsu, C. D. Fassnacht, S. Hilbert, and L. V. E. Koopmans, *Science* **365**, 1134–1138 (2019), 1909.06712.
- [175] S. Birrer et al., *Mon. Not. Roy. Astron. Soc.* **484**, 4726 (2019), 1809.01274.
- [176] C. E. Rusu et al., *Mon. Not. Roy. Astron. Soc.* **498**, 1440 (2020), 1905.09338.
- [177] G. C. F. Chen et al., *Mon. Not. Roy. Astron. Soc.* **490**, 1743 (2019), 1907.02533.
- [178] C. Escamilla-Rivera and R. Torres Castillejos, *Universe* **9**, 14 (2023), 2301.00490.
- [179] K. Akiyama et al. (Event Horizon Telescope), *Astrophys. J. Lett.* **875**, L1 (2019), 1906.11238.
- [180] K. Akiyama et al. (Event Horizon Telescope), *Astrophys. J. Lett.* **930**, L12 (2022), 2311.08680.
- [181] C. Krishnan, E. Ó Colgáin, M. M. Sheikh-Jabbari, and T. Yang, *Phys. Rev. D* **103** (2021), ISSN 2470-0029, URL <http://dx.doi.org/10.1103/PhysRevD.103.103509>.
- [182] A. G. Riess, S. Casertano, W. Yuan, L. M. Macri, and D. Scolnic, *Astrophys. J.* **876**, 85 (2019), 1903.07603.